

Journal of Dental Research

Notch coordinates periodontal ligament maturation through regulating Lamin A

Journal:	<i>Journal of Dental Research</i>
Manuscript ID	JDR-19-0375.R2
Manuscript Type:	Research Reports
Date Submitted by the Author:	31-Jul-2019
Complete List of Authors:	Denes, Balazs; Universite de Geneve, Orthodontics Bolton, Chloe; Peninsula Dental School Illsley, Charlotte; Peninsula Dental School Kok, Wai Ling; Peninsula Dental School Walker, Jemma; Plymouth University Peninsula Schools of Medicine & Dentistry, Peninsula Dental School Poetsch, Ansgar ; University of Plymouth, School of Biomedicine, Faculty of Medicine and Dentistry Tredwin, Christopher; Peninsula Dental School Kiliaridis, Stavros; Univ. Geneve, , Dept Orthodontics Hu, Bing; Peninsula Dental School,
Keywords:	Tooth development, Periodontal ligament (PDL), Occlusion, Molecular biology, Cell biology
Abstract:	Tooth eruption is a continuous biological process with dynamic changes at cellular and tissue levels particularly within the periodontal ligament (PDL). Occlusion completion is a significant physiological landmark of dentition establishment. However the importance of the involvement of molecular networks engaging in occlusion establishment on the final PDL maturation are still largely unknown. In this study, using rat and mouse molar teeth and a human PDL cell line for RNAseq and proteomic analysis, we systematically screened the key molecular links in regulating PDL maturation before and after occlusion establishment. We discovered Notch, a key molecular pathway in regulating stem cell fate and differentiation, is a major player in the event. Intercepting Notch pathway by deleting its key canonical transcriptional factor: RBP-Jkappa using conditional knock out strategy in the mice delayed PDL maturation. We also identified that Lamin A, a cell nuclear lamina member, is one unique marker of PDL maturation and its expression is under the control of Notch signalling. Our study therefore provides a deep insight of how PDL maturation is regulated at molecular level and we expect the outcomes to be applied for a better understanding of the molecular regulation networks in physiological conditions such as tooth eruption and movement, and also for periodontal diseases.

1
2
3
4 SCHOLARONE™
5 Manuscripts
6
7
8
9
10
11
12
13
14
15
16
17
18
19
20
21
22
23
24
25
26
27
28
29
30
31
32
33
34
35
36
37
38
39
40
41
42
43
44
45
46
47
48
49
50
51
52
53
54
55
56
57
58
59
60

1
2
3 **Date submitted: 4/19/2019**
4 **Date last revised: 7/31/2019**
5 **Date accepted: 8/2/2019**
6
7
8
9

10 **Notch coordinates periodontal ligament maturation through regulating Lamin A** 11 12 13

14 Balazs Jozsef Denes¹, Chloe Bolton², Charlotte Sara Illsley², Wai Ling Kok², Jemma Victoria
15 Walker², Ansgar Poetsch³, Christopher Tredwin², Stavros Kiliaridis¹, Bing Hu^{2*}
16
17

18 1. Department of Orthodontics, University Clinic of Dental Medicine, University of Geneva,
19
20
21 Genève 4 CH, Rue Michel-Servet 1, 1211, Switzerland
22
23
24

25 2. Stem Cells & Regenerative Medicine Laboratory, Peninsula Dental School, Faculty of
26 Medicine and Dentistry, University of Plymouth, 16 Research Way, Plymouth, PL6 8BU,
27
28 United Kingdom
29
30

31 3. School of Biomedicine, Faculty of Medicine and Dentistry, University of Plymouth, 16
32 Research Way, Plymouth, PL6 8BU, United Kingdom
33
34
35

36
37
38
39
40
41
42
43
44 *Corresponding author
45
46 Prof. Bing Hu: bing.hu@plymouth.ac.uk
47
48
49
50
51
52
53
54
55
56
57
58
59
60

Running title: Notch controls periodontal ligament development

Key words: Tooth; Periodontal ligament; Occlusion; Notch, Lamin A

1
2
3
4
5
6
7
8
9
10
11
12
13
14
15
16
17
18
19
20
21
22
23
24
25
26
27
28
29
30
31
32
33
34
35
36
37
38
39
40
41
42
43
44
45
46
47
48
49
50
51
52
53
54
55
56
57
58
59
60

For Peer Review

Abstract

Tooth eruption is a continuous biological process with dynamic changes at cellular and tissue levels particularly within the periodontal ligament (PDL). Occlusion completion is a significant physiological landmark of dentition establishment. However the importance of the involvement of molecular networks engaging in occlusion establishment on the final PDL maturation are still largely unknown. In this study, using rat and mouse molar teeth and a human PDL cell line for RNAseq and proteomic analysis, we systematically screened the key molecular links in regulating PDL maturation before and after occlusion establishment. We discovered *Notch*, a key molecular pathway in regulating stem cell fate and differentiation, is a major player in the event. Intercepting *Notch* pathway by deleting its key canonical transcriptional factor: *RBP-Jkappa* using conditional knock out strategy in the mice delayed PDL maturation. We also identified that *Lamin A*, a cell nuclear lamina member, is one unique marker of PDL maturation and its expression is under the control of *Notch* signalling. Our study therefore provides a deep insight of how PDL maturation is regulated at molecular level and we expect the outcomes to be applied for a better understanding of the molecular regulation networks in physiological conditions such as tooth eruption and movement, and also for periodontal diseases.

Introduction

Tooth eruption is accompanied by the development and maturation of PDL (Cho and Garant 2000). Recent studies suggest PDL originates from dental follicle progenitors that can be either *Osx Cre* (Ono et al. 2016) and/or *PTHrP-Cre* positive (Takahashi et al. 2019). During pre-occlusal eruption phase, a tooth performs axial movement till occlusion is reached, as such no exogenous tension or compression forces are applied on PDL yet. In parallel to the tooth eruption, mesenchymal cells inside PDL secrete increasing amounts of extracellular matrix such as collagen and elastin, which further polymerise into collagen fibres and elastic fibres (Berkovitz and Moxham 1990). Upon contacting the opposite tooth, i.e. the occlusion is established and root development is completed. The PDL fibres are then organized into thick bundles and suspend the tooth in the alveolar socket, hence are under the challenge of constant stretching force, facilitating the tooth to adapt to the biting force and prevent tissue damages (Beertsen et al. 1997).

The molecular networks and mechanisms linking occlusion establishment with PDL development has not been previously systemically screened yet. In many systems, *Notch* signalling plays a key role in controlling stem cell maintenance and differentiation (Cheung and Rando 2013). Notch proteins are transmembrane receptors that act through cell-to-cell and cell-to-matrix signalling (Giaimo and Borggreffe 2018). Binding of Notch receptor to ligand leads to the cleavage of the receptor's intramembrane sites and releasing of the intracellular domain (ICD), which translocates into nucleus and binds to the RBP-Jkappa transcription effector complex. Notch receptors are also sensitive to extracellular forces, and a small amount of force can reveal the S2 cleavage site for proteinases, which leads to release of the ICD domain and gene transcription (Kopan and Ilagan 2009). In the tooth, increasing evidence suggests that *Notch* is essential in the pulp and cervical loop stem cell maintenance and terminal odontoblast differentiation, as well as in tooth pulp wound healing ((Kurpinski et al. 2010;

Lovschall et al. 2007), and Walker et al., in press). However, although *Notch* pathway has been implicated in inducing osteogenic differentiation of cultured PDL cells (Li et al. 2014; Nakao et al. 2009; Osathanon et al. 2013), its function in periodontal ligament development and particularly maturation has not been elucidated.

In this study, we provide novel *in vivo* and *in vitro* evidence highlighting the important role of *Notch* pathway in periodontal ligament development and maturation with nuclear lamina protein *Lamin A* as a direct target.

Materials & Methods

Animals

The Wistar rat and tooth eruption stages were determined based on data of a previous study (Denes et al. 2018) and verified by micro-CT scans. The work was approved by the ethics committee of animal research of the Canton of Geneva (n° GE/72/15). *RBP-Jκappa*^{loxP/loxP} and *Collα2-Cre* mice are as reported previously (Hu et al. 2010).

Laser capture microdissection

Mandibles were dissected and immediately frozen in PrestoChill (Milestone, Type 51420) at -40°C and stored at -80°C. Sections were performed with a cryostat and transferred to PET-membrane slides with the CryoJane Tape system (Leica Biosystems). Slides were dehydrated successively with 70%, 95%, 100% EtOH at -20°C. Microdissection of the periodontal ligament (PDL) was performed at the cervical 1/3 PDL region. For each developmental stage, 4 individual animals were used.

RNAseq statistical analysis

RNA extraction was performed according to RNeasy Micro Kit (Qiagen®). RNA quantity and quality was evaluated with Agilent 2100 Bioanalyzer (Agilent Technologies). RIN number

equal or greater to 7 was required for the sample for analysis. Total RNA was amplified and Next-Generation Sequencing with the Illumina HiSeq 4000 was performed with protocol Smarter + Nextera and the reference genome Rattus Norvegicus. Quality was assessed by FastQC v.0.11.5 and resulted in values between 32 and 40 (error: 1/1'000 to 1/10'000). The reads (length=100 bp) were mapped with the STAR v2.5.3a software to the reference genome and showed good alignment percentage ($71.7\% \pm 5.9$). Biological quality control and summarization were done with the PicardTools v2.9.0 with percentage of mRNA bases as average 63%. The normalization and differential expression analysis was performed with the R/Bioconductor package edgeR v.3.16.5 and statistical significance was assessed with General Linear Model, negative binomial distribution and a quasi-likelihood *F*-test. Threshold for significance was set at p-value <5% and fold change (FC)>1.5. The RNAseq data can accessed through number: GSE129458 from <https://www.ncbi.nlm.nih.gov/geo/>. Enrichment analysis of RNAseq was performed with GO Ontology database and analyzed with PANTHER Overrepresentation Test. Fischer test was used with false discovery rate (FDR) correction applied. Biological processes, molecular functions and cell compartment analyses were classified based number of genes.

Rat paraffin sections

The cryoembedded mandibles were washed in distilled water to remove MCC, fixed in 4% paraformaldehyde (Merck), decalcified in Osteosoft (Sigma-Aldrich) or 14% EDTA (pH7.4) for a period of 6-weeks, embedded in paraffin. The paraffin blocks were cut into sections of 3 μ m thickness at the second root-pair of the first molar for rat samples and 10 μ m for mouse teeth.

Immunohistochemistry/Immunofluorescence

1
2
3 4-5 individual animals were used for each genotype at each defined stage. Osteosoft (Sigma-
4 Aldrich) or 14% EDTA (pH7.4) decalcified samples were cut into 3 μ m thickness sections. The
5 sections were deparafinized and antigen retrieval was done in citrate buffer (pH8.0) at 98°C
6 for 20 min or a microwave at 750w for 1 minute, followed by blocking in PBS containing 5%
7 donkey serum, 0.25% cold water fish gelatine and 0.25% bovine serum albumin for 1h at room
8 temperature and incubated with primary antibodies for overnight at 4°C, and secondary
9 antibodies for 2h at room temperature. and counterstained with 4'-6-diamidino-2-phenylindole
10 (DAPI). Imaging was performed with a Leica DMI6000 confocal microscope. For
11 immunohistochemistry, Vectastain with DAB substrate were used. For details please see
12 Appendix Table 3. Goldner staining was used for collagen staining.
13
14
15
16
17
18
19
20
21
22
23
24
25
26
27
28
29
30
31
32
33
34
35
36
37
38
39
40
41
42
43
44
45
46
47
48
49
50
51
52
53
54
55
56
57
58
59
60

Cell cultures and treatment

Human periodontal ligament fibroblasts (hPLF, ScienCell, Catalog #2630) were cultured in DMEM/F-12 with 20% FBS and 1% Antibiotic-Antimycotic. For Jagged1 treatment, after overnight seeding and cell confluence reached to 70%, Jagged1 was added to the medium to reach to a final concentration of 100ng/ml. Cultures were fixed after 24h of Jag1 treatment with 4% PFA at room temperature for 20 minutes and then washed 2x with PBS (10mM).

Stretching experiments were performed with the stretching device and silicone membranes (Strex USA, ST-140-04) (Appendix Figure 1 and 2). The membranes were coated with rat tail collagen type I (Life Technologies, A1048301) and HCl at 1:1 ratio overnight at 37°C. Cells were seeded as 2x10⁵ cells per membrane. Cells were stretched for 6h, 12h and 24h at 37°C alongside controls.

Quantitative real-time RT-PCR

Tirpilated samples were used for each gene analysis. Total RNAs was extracted using the penol-chloroform technique and reverse transcription of was achieved with High-Capacity cDNA synthesis kit (Thermo Fisher Scientific), as previously described (Singer et al. 2019). The PCR reaction was performed with SYBR Green I Master Mix (Roche) on a LightCycler 480 II Real-Time PCR system (Roche Molecular Diagnostics) for 45 cycles. *36 beta4* gene was used as housekeeping gene to normalize samples with the $2^{-\Delta\Delta Ct}$ method. All analyses were performed with three replicates as described previously (Hu et al. 2012). For the primers used in this study please see Appendix Table 3.

Nanoscale Liquid Chromatographic–Electrospray Ionization–Tandem Mass Spectrometry (nLC–ESI–MS/MS)

Duplicated samples were used for the analysis. In-gel tryptic digestion of proteins was carried out as described in (Costa et al. 2018). Peptides were separated on an HSS T3 column (waters) and injected into an Orbitrap Elite MS using a 90 min gradient from 2 to 30% acetonitrile, 0.1% formic acid. Full MS scans in the orbitrap and fragmentation of 20 most intense precursors in parallel was done. Protein identification and label-free quantification was done with MaxQuant (Cox et al. 2014) and further statistical analysis with Perseus (Tyanova et al. 2016). Differential expression of fold change > 2 was analyzed with Gene Ontology (GO) enrichment of biological processes powered by Panther Database (pantherdb.org) and clustering was performed with String Database v11.0 (string-db.org). For *in vivo* proteomic analysis, electrospray ionization Liquid-Chromatography-Mass Spectrometry/Mass Spectrometry (ESI-LC-MSMS) was performed on rat mandible periodontal ligament, dissected with laser capture microdissection

1
2
3 technique. The results can be access with number: PXD013379 from
4
5 https://www.ebi.ac.uk/pride/archive/.
6
7
8
9
10

11 Western Blotting 12

13 Cells were washed with HBSS, collected at 10,000 rpm for 10 minutes at 4°C. The pellet was
14 re-suspended in ice-cold radioimmunoprecipitation assay buffer (89901, Pierce) with protease
15 & phosphatase inhibitor cocktail (78442, Pierce) and incubated on ice for 30 minutes then spun
16 down at 10,000rpm for 10 minutes at 4°C. The supernatant was collected and quantified with
17 BCA method (23225, Pierce). Protein were separated with 4-12% NuPAGE Novex Bis-Tris
18 gel and transferred to polyvinylidene membrane, detected with iBind Flex Western device
19 (SLF2000S, Invitrogen). Antibodies were diluted in iBindFlex solution (SLF2020, Invitrogen).
20 Membranes were scanned with C-DiGit scanner (Li-COR, 3600-00). For antibodies see
21 Appendix Table 3.
22
23
24
25
26
27
28
29
30
31
32
33
34
35
36
37
38
39
40
41
42
43
44
45
46
47
48
49
50
51
52
53
54
55
56
57
58
59
60

Results

PDL has distinct gene expression profile changes upon occlusion establishment

We selected postnatal day 18 (P18, pre-occlusion eruption) and 28 (P28, 1 week after occlusion establishment) of the Wistar rat's second root pair of the first lower molar as the studying models. The eruption stage was confirmed by daily *in vivo* micro-CT imaging based on our previous study (Denes et al. 2018). Histological analysis and micro-CT confirmed that the root development of P18 tooth was at the initial elongation stage, while at P28 the root development reached near completion (Figure 1A and Appendix Figure 1A). Trichrome staining showed P28 PDL was abundant with collagen fibres, comparing to P18 (Figure 1B). As well, P28 PDL expressed significantly higher level of Periostin (Figure 1C). To explore the transcriptome changes of PDL, we next performed RNAseq analysis on the PDL at indicated

1
2
3 stages (RNAseq accession number: GSE129458). Among a total of 12,742 detected genes, we
4 identified 1,090 genes were upregulated and 1,035 were downregulated with more than 1.5
5 fold changes with p value < 5%, at P28 comparing to P18 (Appendix Table 1). Gene enrichment
6 analysis suggested P28 has significantly increased cellular process and protein binding events
7 comparing to P18 (Figure 1D). Heatmap of genes identified by Metacore pathway map analysis
8 shows consistent expression throughout samples (Figure 1E). Using GO analysis to examine
9 the biological processes and Metacore process networks, as expected, we have identified that
10 “biomineral tissue development” and “muscle contraction” are among the most significantly
11 changed biological processes (Figure 1F and Appendix Figure 1B).

23 24 25 26 **Notch signalling is dynamically changed before and after occlusion is established**

27
28 String analysis suggested *Notch* pathway acted as a center of the molecular networks (Figure
29 2A). Metacore pathway map analysis further confirmed *PI3K* and *Notch* signalings are the top
30 two pathways affected (Figure 2B). As the function of *Notch* signaling has not been described
31 previously in PDL *in vivo*, particularly in the occlusion establishing stage, we therefore
32 continued focusing on that pathway for our study.

33
34 In the RNAseq analysis, *Notch1*, *Notch4* and *Dll1* are the *Notch* pathway members that
35 were significantly upregulated in the P28 PDL comparing to P18 ($p<0.05$), and *Jagged 1* was
36 upregulated with a marginal p value ($p = 0.067$), and *Furin* was significantly downregulated
37 ($p<0.05$) (Figure 2C). We next compared Notch protein expression with immunofluorescence
38 analysis. Consistent with the RNAseq results, we found that both total *Notch1* and its ICD were
39 increasingly expressed in the P28 PDL (Figure 2D and E) as well as Notch ligands such as *Dll1*
40 (Figure 2F), in parallel to the increased PDL maturation marker: Osteopontin (Figure 2G) (Rios
41 et al. 2008). Interestingly, when we evaluated in parallel the other Notch receptor, *Notch2*
42 ICD's expression was at its highest level at pre-occlusal eruption stage and decreased thereafter
43
44
45
46
47
48
49
50
51
52
53
54
55
56
57
58
59
60

(Figure 2H), suggesting that Notch1 and Notch2 receptors play significant however different roles in PDL development.

Intercepting Notch pathway delays PDL development and tooth eruption

To confirm the function of *Notch* pathway in PDL development during occlusion establishment, we adopted the mesenchymal conditional *RBP-Jkappa* knockout transgenic mouse model, where the *Cre* recombinase expression is under the control of *Collagen 1 α2* promoter (Hu et al. 2010). Staining with specific antibodies, we observed abundant Cre protein expression in the PDL cells confirmed the deletion of the *RBP-Jkappa* gene in PDL cells, as well as osteoblasts at the bone surface (Figure 3A). By crossing the *Collagen 1 α2 Cre* transgenics with *RBP-Jkappa*^{fl/fl} mice (Hu et al. 2012; Hu et al. 2010), phenotypically at P21 when the tooth eruption is complete in the WT mice, the mice with *RBP-Jkappa* deletion in PDL cells encountered significant delay of tooth eruption and root development (Figure 3B). Macroscopy analysis revealed the *RBP-Jkappa* knockout mice had smaller mandibles (Figure 3C) and molar crown size. (Figure 3D). Stereomicroscopy and microCT analysis and quantification (Figure 3G) suggested that while initially the root development is delayed in the *RBP-Jkappa* knockout mice (Figure 3E and G), the tooth crown eruption in the mutants could still be eventually completed (Figure 3F) and root length had no difference comparing the control with the knockout mice (Figure 3G). Consistently, immunofluorescence analysis on Periostin expression suggested at P4 there were no expression of the marker (Appendix Figure 2A), while at P10 and P14 the knockout mice has a significantly delayed expression (Figure H&I). However, after two months there are no notable difference between the control and knockout animals' PDL (Figure 2J).

In vitro stretching mirrored occlusion establishment effects on PDL cells

To confirm if the key molecular changes identified in the *in vivo* RNAseq analysis were due to the stretching of PDL mesenchymal cells and its relevance to human, we next cultured human PDL cells and mimicked occlusive stretching force by inducing reciprocal force on the cells on an automatic cell stretching system (Appendix Figure 2B and C). Real-Time RT-PCR results confirmed significant induction of the mRNA expression of *Notch* pathway members such as *Jagged 1*, *Dll1* and *Hey1* (Figure 4A), as well a panel PDL cell differentiation markers including Osteopontin (Figure 4B). To further gain insight of the molecular targets of the PDL in responding to stretching force, we performed proteomic analysis on the stretched PDL cells and found extracellular matrix protein such as collagen and periostin and the RhoA-CDC42 associated cytoskeleton regulating system were significantly changed (Figure 4C and D, and Appendix Table 2).

Lamin A is a direct effector in PDL in responding to stretching and act as Notch downstream target

By comparing the *in vitro* PDL cell stretching results with proteomic analysis from the *in vivo* PDL maturation (PRIDE number: PXD013379) and RNAseq analysis, we noticed the nuclear membrane protein: Lamin A was the only molecule displaying the same upregulation pattern across the three analyses (Figure 5A). Immunofluorescent analysis confirmed that Lamin A/C expression did increase in the P28 rat PDL, comparing with P18 samples (Figure 5B). Western Blot analysis suggested Lamin A protein level is specifically induced in the stretched human PDL cells but not Lamin C (Figure 5C). Similarly, treating PDL cells with Notch ligand: Jagged1 could induce Lamin A expression (Figure 5D). Finally, in the *RBP-J kappa* knockout mice PDL, Lamin A/C expression was concomitantly reduced both at P10 and 2 months (Figure 5E and F). Therefore, *Lamin A* is indeed an indicator of PDL maturation that is under *Notch* signalling control and is positively regulated by stretching force.

Discussion

The development of PDL, alveolar bone and cementum are closely linked events. So far, particularly for PDL and alveolar bone, it is still a dearth for finding genetic tools to dissect the specific populations inside the tissues, particularly for fibroblasts and osteoblasts. However, increasing evidence have already shown that multiple signalling pathways are closely involved in the periodontium development, such as *NFI-C* null mice abolish root development (Steele-Perkins et al. 2003) and conditional deletion of *Smad4* in tooth epithelium can impede root growth (Li et al. 2015), while conditional deletion PPR using PTHrP-Cre impede tooth eruption (Takahashi et al. 2019). *Notch* signalling is one of the key pathways in determining mesenchymal stem cell fate and cell differentiation such as in the muscles (Conboy et al. 2003; Conboy and Rando 2002). In bone and bone marrow mesenchymal progenitors, *Notch*'s function has been extensively described in protecting mesenchymal progenitors (Hilton et al. 2008). While in the tooth, previous reports and our findings suggest that *Notch* is important both for maintaining stem cells and differentiation but the functions are carried out via different Notch receptors: i.e. *Notch1* acts through maintaining stem cell pool and inducing cell differentiation and *Notch2* is rather responsible for maintaining transit amplifying cells ((Mitsiadis et al. 2017; Zhang et al. 2008) and Walker et al. in press). In PDL, our results confirm that *Notch1* is linked with PDL final development and completion, while interestingly *Notch2* preferentially functions during the pre-occlusion stage. This might reflect a different role of *Notch2* in enhancing cell populating into the tissue, similar to the findings in the incisor mesenchymal stem cells (Walker et al. in press). Although we have not been able to achieve the mesenchymal specific conditional Notch receptor deletion models due to early death in embryonic stages (data not shown), it would be still interesting to apply inducible conditional deletion models to distinguish the different roles of Notch receptors in PDL development. As

well, future studying Notch's roles such as in PDL stem cell fate control, as well as aging are highly desired (Appendix Figure 3).

In addition, our results showed that blocking canonical *Notch* pathway by deleting *RBP-Jkappa* in the PDL delayed but did not inhibit tooth eruption and PDL maturation completely, suggesting that canonical *Notch* is dispensable in these events. Significantly, the Notch ligands: *Dll1*, *Dll4* and *Jagged1* expression are all highly elevated in the PDL cells upon stretching, suggesting the PDL cells play a central role in the tissue homeostasis, possibly through *Notch* pathway ligands production, to affect surrounding microenvironment, such as vascularisation through endothelial cell specific Notch4 receptor. One evidence to support this theory is that during orthodontic tooth movement, blood vessel proliferation and remodelling is among the early key events in the PDL (Rygh et al. 1986; Vandevska-Radunovic et al. 1994).

Lamin A is an important nuclear envelope molecule for protecting cells from DNA damage and pre-aging and its mutation can cause laminopathies including Progeria (Broers et al. 2006; Eriksson et al. 2003; Worman 2012). Lamin A gene encodes two isoforms: Lamin A and C that are created from alternative splicing that encode important protein for nuclear envelopes. While Lamin C is shorter and produced directly, Lamin A, which is two exons longer at C-terminal, is required to pass prelamin A stage followed by a series of posttranslational modifications initiated from the farnesylation of C terminal cysteine (Lin and Worman 1993). We observed Lamin A transcription and translation were both elevated upon occlusion establishment, as well as under stretching condition in the PDL cells, which indicates its potential significant role in protecting the cells from stretching force induced cellular damages. The evidence that *Notch* signal activation by Jagged1 treatment could also elevate Lamin A but not Lamin C expression further confirmed that Lamin A potentially has significant role in PDL development and homeostasis, which requires additional investigations.

We hope our study is opening a new gateway and molecular clues for understanding how the PDL, one of the most dynamically changed tissues in the body, is maintained for homeostasis and integrity, not only in physiological conditions, but also for periodontal diseases.

Acknowledgement

We would like to thank the helps provided by platforms of the University of Geneva, including the iGE3 Genomics Platform, the Bioimaging Core Facility, the Histology Core Facility. This study was supported by the Swiss National Science Foundation grant n° FNRS 31003A_176131/1 to S. K., the European Union Marie Skłodowska-Curie Actions (618930, OralStem FP7-PEOPLE-2013-CIG), the European Regional Development Fund and the Biotechnology and Biological Sciences Research Council of the UK (BB/L02392X/1) to B.H. B.D., S.K. and B.H. contributed to conception and design of the work. B.D. and B.H. drafted the manuscript. B.D., C.B., C.I., W.K., J.W., A.P. and B.H. contributed to the acquisition and analysis of the data. C.T. and S.K. contributed to the interpretation of the data. All the authors critically revised the manuscript. The authors declare that there is no conflict of interest regarding the publication of this article.

Material and data availability statement

The materials used and datasets generated during and/or analysed during the current study are available from the corresponding author on reasonable request.

Reference

Beertsen W, McCulloch CA, Sodek J. 1997. The periodontal ligament: A unique, multifunctional connective tissue. *Periodontol 2000*. 13:20-40.

- 1
2
3 Berkovitz BK, Moxham BJ. 1990. The development of the periodontal ligament with special
4 reference to collagen fibre ontogeny. *J Biol Buccale*. 18(3):227-236.
5
6 Broers JL, Ramaekers FC, Bonne G, Yaou RB, Hutchison CJ. 2006. Nuclear lamins:
7
8 Laminopathies and their role in premature ageing. *Physiol Rev*. 86(3):967-1008.
9
10 Cheung TH, Rando TA. 2013. Molecular regulation of stem cell quiescence. *Nat Rev Mol Cell
11 Biol*. 14(6):329-340.
12
13 Cho MI, Garant PR. 2000. Development and general structure of the periodontium. *Periodontol
14 2000*. 24:9-27.
15
16 Conboy IM, Conboy MJ, Smythe GM, Rando TA. 2003. Notch-mediated restoration of
17 regenerative potential to aged muscle. *Science*. 302(5650):1575-1577.
18
19 Conboy IM, Rando TA. 2002. The regulation of notch signaling controls satellite cell activation
20 and cell fate determination in postnatal myogenesis. *Dev Cell*. 3(3):397-409.
21
22 Costa MI, Cerletti M, Paggi RA, Trotschel C, De Castro RE, Poetsch A, Gimenez MI. 2018.
23
24 Haloferax volcanii proteome response to deletion of a rhomboid protease gene. *J
25 Proteome Res*. 17(3):961-977.
26
27 Cox J, Hein MY, Luber CA, Paron I, Nagaraj N, Mann M. 2014. Accurate proteome-wide
28 label-free quantification by delayed normalization and maximal peptide ratio
29 extraction, termed maxlfq. *Mol Cell Proteomics*. 13(9):2513-2526.
30
31 Denes BJ, Lagou A, Dorotheou D, Kiliaridis S. 2018. A longitudinal study on timing and
32 velocity of rat molar eruption: Timing of rat molar eruption. *Lab Anim*. 52(4):394-401.
33
34 Eriksson M, Brown WT, Gordon LB, Glynn MW, Singer J, Scott L, Erdos MR, Robbins CM,
35 Moses TY, Berglund P et al. 2003. Recurrent de novo point mutations in lamin a cause
36 hutchinson-gilford progeria syndrome. *Nature*. 423(6937):293-298.
37
38 Giaimo BD, Borggrefe T. 2018. Introduction to molecular mechanisms in notch signal
39 transduction and disease pathogenesis. *Adv Exp Med Biol*. 1066:3-30.

- Hilton MJ, Tu X, Wu X, Bai S, Zhao H, Kobayashi T, Kronenberg HM, Teitelbaum SL, Ross FP, Kopan R et al. 2008. Notch signaling maintains bone marrow mesenchymal progenitors by suppressing osteoblast differentiation. *Nat Med.* 14(3):306-314.
- Hu B, Castillo E, Harewood L, Ostano P, Reymond A, Dummer R, Raffoul W, Hoetzenrecker W, Hofbauer GF, Dotto GP. 2012. Multifocal epithelial tumors and field cancerization from loss of mesenchymal csl signaling. *Cell.* 149(6):1207-1220.
- Hu B, Lefort K, Qiu W, Nguyen BC, Rajaram RD, Castillo E, He F, Chen Y, Angel P, Brisken C et al. 2010. Control of hair follicle cell fate by underlying mesenchyme through a csl-wnt5a-foxn1 regulatory axis. *Genes Dev.* 24(14):1519-1532.
- Kopan R, Ilagan MX. 2009. The canonical notch signaling pathway: Unfolding the activation mechanism. *Cell.* 137(2):216-233.
- Kurpinski K, Lam H, Chu J, Wang A, Kim A, Tsay E, Agrawal S, Schaffer DV, Li S. 2010. Transforming growth factor-beta and notch signaling mediate stem cell differentiation into smooth muscle cells. *Stem Cells.* 28(4):734-742.
- Li J, Feng J, Liu Y, Ho TV, Grimes W, Ho HA, Park S, Wang S, Chai Y. 2015. Bmp-shh signaling network controls epithelial stem cell fate via regulation of its niche in the developing tooth. *Dev Cell.* 33(2):125-135.
- Li Y, Li SQ, Gao YM, Li J, Zhang B. 2014. Crucial role of notch signaling in osteogenic differentiation of periodontal ligament stem cells in osteoporotic rats. *Cell Biol Int.* 38(6):729-736.
- Lin F, Worman HJ. 1993. Structural organization of the human gene encoding nuclear lamin A and nuclear lamin C. *J Biol Chem.* 268(22):16321-16326.
- Lovschall H, Mitsiadis TA, Poulsen K, Jensen KH, Kjeldsen AL. 2007. Coexpression of notch3 and rgs5 in the pericyte-vascular smooth muscle cell axis in response to pulp injury. *Int J Dev Biol.* 51(8):715-721.

- Mitsiadis TA, Caton J, Pagella P, Orsini G, Jimenez-Rojo L. 2017. Monitoring notch signaling-associated activation of stem cell niches within injured dental pulp. *Front Physiol.* 8:372.
- Nakao A, Kajiya H, Fukushima H, Fukushima A, Anan H, Ozeki S, Okabe K. 2009. PthrP induces notch signaling in periodontal ligament cells. *J Dent Res.* 88(6):551-556.
- Ono W, Sakagami N, Nishimori S, Ono N, Kronenberg HM. 2016. Parathyroid hormone receptor signalling in osterix-expressing mesenchymal progenitors is essential for tooth root formation. *Nat Commun.* 7:11277.
- Osathanon T, Manokawinchoke J, Nowwarote N, Aguilar P, Palaga T, Pavasant P. 2013. Notch signaling is involved in neurogenic commitment of human periodontal ligament-derived mesenchymal stem cells. *Stem Cells Dev.* 22(8):1220-1231.
- Rios HF, Ma D, Xie Y, Giannobile WV, Bonewald LF, Conway SJ, Feng JQ. 2008. Periostin is essential for the integrity and function of the periodontal ligament during occlusal loading in mice. *J Periodontol.* 79(8):1480-1490.
- Rygh P, Bowling K, Hovlandsdal L, Williams S. 1986. Activation of the vascular system: A main mediator of periodontal fiber remodeling in orthodontic tooth movement. *Am J Orthod.* 89(6):453-468.
- Singer D, Thamm K, Zhuang H, Karbanova J, Gao Y, Walker JV, Jin H, Wu X, Coveney CR, Marangoni P et al. 2019. Prominin-1 controls stem cell activation by orchestrating ciliary dynamics. *EMBO J.* 38(2).
- Steele-Perkins G, Butz KG, Lyons GE, Zeichner-David M, Kim HJ, Cho MI, Gronostajski RM. 2003. Essential role for nfi-c/ctf transcription-replication factor in tooth root development. *Mol Cell Biol.* 23(3):1075-1084.
- Takahashi A, Nagata M, Gupta A, Matsushita Y, Yamaguchi T, Mizuhashi K, Maki K, Ruellas AC, Cevidanes LS, Kronenberg HM et al. 2019. Autocrine regulation of mesenchymal

1
2
3 progenitor cell fates orchestrates tooth eruption. Proc Natl Acad Sci U S A. 116(2):575-
4
5 580.
6
7

8 Tyanova S, Temu T, Sinitcyn P, Carlson A, Hein MY, Geiger T, Mann M, Cox J. 2016. The
9 perseus computational platform for comprehensive analysis of (prote)omics data. Nat
10 Methods. 13(9):731-740.
11
12

13 Vandevska-Radunovic V, Kristiansen AB, Heyeraas KJ, Kvinnslund S. 1994. Changes in
14 blood circulation in teeth and supporting tissues incident to experimental tooth
15 movement. Eur J Orthod. 16(5):361-369.
16
17

18 Walker JV, Zhuang H, Singer D, Illsley CS, Kok WL, Sivaraj KK, Gao Y, Bolton C, Liu Y,
19 Zhao M et al. 2019. Transit amplifying cells coordinate mouse incisor mesenchymal
20 stem cell activation. Nature Communications. In press. **(Needs update prior to
21 publication)
22
23

24 Worman HJ. 2012. Nuclear lamins and laminopathies. J Pathol. 226(2):316-325.
25
26

27 Zhang C, Chang J, Sonoyama W, Shi S, Wang CY. 2008. Inhibition of human dental pulp stem
28 cell differentiation by notch signaling. J Dent Res. 87(3):250-255.
29
30
31
32
33
34
35
36
37
38
39
40
41
42
43
44
45
46
47
48
49
50
51
52
53
54
55
56
57
58
59
60

Figure legends**Figure 1. PDL express distinct molecular signatures upon occlusion establishment**

A: Hematoxylin-Eosin (HE) staining of the P18 and P28 rat first lower molar.

B: Goldner staining of P18 and P28 PDL regions. Note the green-blue stained collagen fibers are abundant at P28 but not P18.

C: Immunofluorescent staining of Periostin with a specific antibody raised in rabbit then visualised using anti-Rabbit Alexa 568 (red) conjugated secondary antibody. Note the significantly increased Periostin signal at P28 comparing to P18.

D: Gene function enrichment analysis on the RNAseq results by comparing P28 with P18 PDL.

E, F: Differential analysis performed on the RNAseq results by comparing P28 with P18 PDL.

E: Metacore Pathway Maps heatmaps analysis.

D: GO analysis for the biological processes.

Bars: A: 100µm; B, C: 20µm.

Figure 2. Notch signalling has dynamic changes during PDL maturation

A: String analysis of the genes of top 10 pathways of the metacore Pathway Maps of the RNAseq results.

B: Metacore Pathway Maps analysis.

C: String analysis of the genes of top 10 pathways of the metacore Pathway Maps.

D: Notch pathway members that had significant changes in the RNAseq analysis.

D-H: Immunofluorescent analysis of the indicated molecules using specific primary antibodies.

The Alexa 488 (green) or 568 (red) conjugated secondaries were used to identify the primary antibodies. Dotted lines mark the boundary between PDL and bone (B) or dentin (D).

Bars: 20 μ m

Figure 3. Intercepting canonical Notch pathway delayed PDL maturation

A: Immunostaining PDL of the second lower molars from P21 RBP-Jk^{flox/flox} (control) and Collagen 1a2 Cre x RBP-Jk^{flox/flox} (cKO) mice. Note the Cre positive signal could only be observed in the cKO mice.

B: HE staining of the P21 control and cKO mice second lower molars. Stars: PDL.

C, D: Stereo images of 1 month old control and cKO mouse mandibles and first lower molars.

Note the cKO mouse tooth's crown size are smaller and roots are shorter than the control.

E: Representative stereo images of the first and third lower molars of the control and cKO mice at postnatal day 14.

F: Representative micro-CT analysis of the control and cKO fist lower molar eruption from 4 months old animals.

G: First lower molar mesial buccal root length comparisation at P14 and 2 months. ** p<0.01.

H-J: Immunofluorescent analysis of Periostin using specific primary followed by secondary antibodies (Alexa 568, red) at indicated stages. Note comparing to the controls, RBP-Jkappa cKO mouse PDL has delayed expression of Periostin at P10 and P14, but not at 2 months.

Bars: A, B, H-J: 20 μ m; C-F: 1mm.

Figure 4. Stretching force induced *Notch* pathway activation and matrix protein productions on a human PDL cell line.

1
2
3 A and B: Real time RT-PCR analysis on human PDL cells at a ratio of 20% stretching and
4 frequency of 30x/min. Samples were collected after 12 hours. ** p<0.01.
5
6

7 C: Metacore analysis of proteomic analysis on the samples of A and B.
8
9

10 D: String analysis of the top 5 pathways affected by stretching force.
11
12
13
14

15 **Figure 5. Lamin A is a marker of PDL maturation and is under the control of Notch
16 pathway.**
17
18

19 A: Compound analysis of the common targets from the *in vivo* RNAseq (Figure 1) and
20 proteomic and *in vitro* cell stretching results (Figure 4). Note Lamin A (LMNA) is the only
21 molecule that was commonly regulated in the three conditions.
22
23

24 B: Immunofluorescent analysis of Lamin A/C expression in the P18 vs. P28 PDL. D: Dentin;
25 B: Bone; Dotted lines: boundaries.
26
27

28 C: Western blotting analysis of Lamin A/C expression in the human PDL cells upon stretching
29 (Figure 4 A&B), with GapDH as the loading control. Note only Lamin A expression was
30 significantly changed.
31
32

33 D: Western blotting analysis of Lamin A/C expression in the human PDL cells treated with
34 Jagged1, with GapDH as the loading control. Note again only Lamin A expression was
35 significantly changed.
36
37

38 E and F: Immunofluorescent analysis of Lamin A/C expression in the control and cKO mouse
39 PDL at P10 and 2 months. D: Dentin; B: Bone; Dotted lines: boundaries.
40
41

42 Bars: 20 μ m
43
44

45
46

47
48

49
50

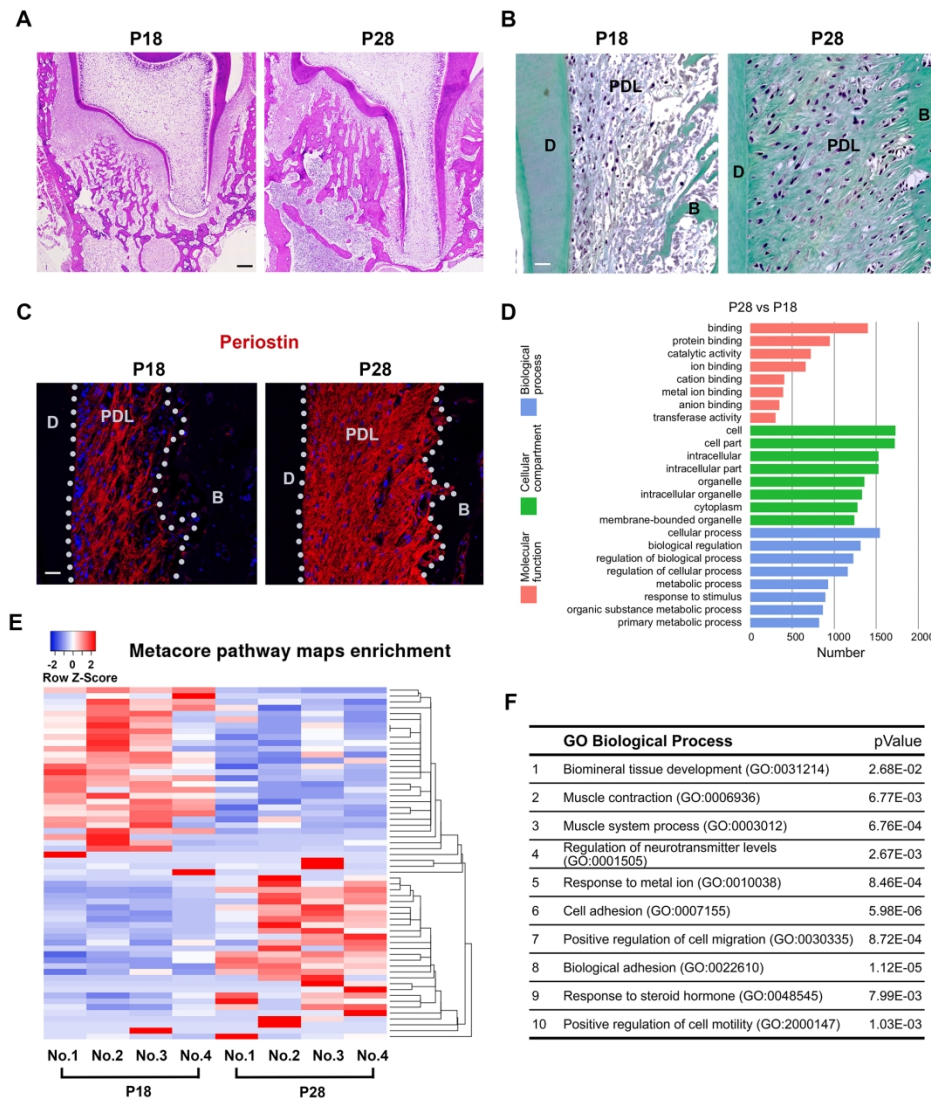
51
52

53
54

55
56

57
58

59
60

**Figure 1**

182x227mm (300 x 300 DPI)

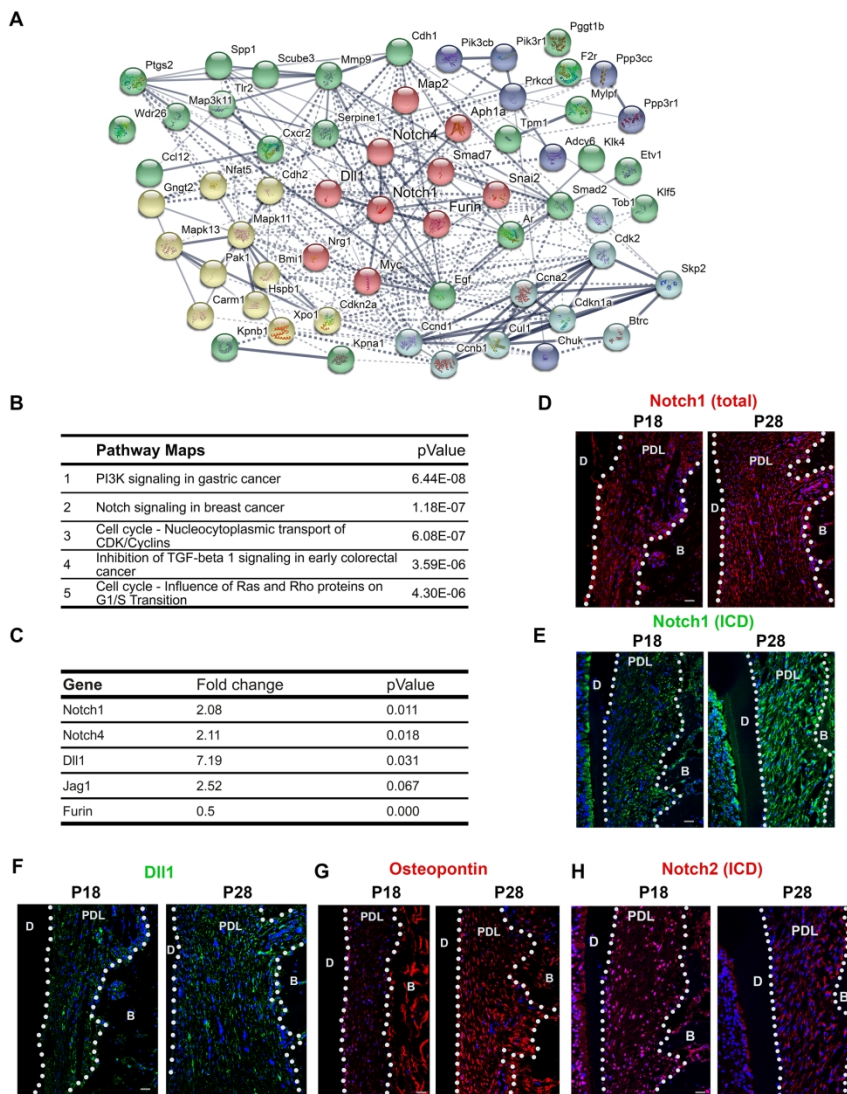


Figure 2

184x252mm (300 x 300 DPI)

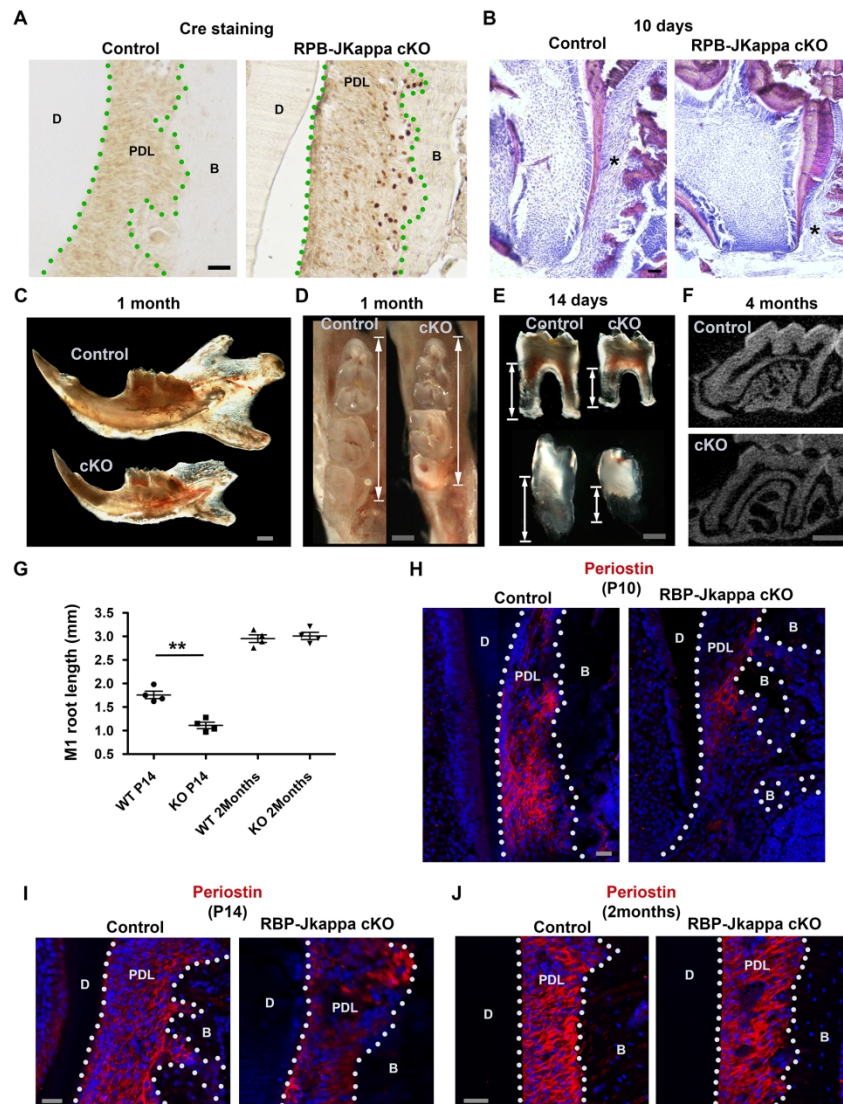


Figure 3

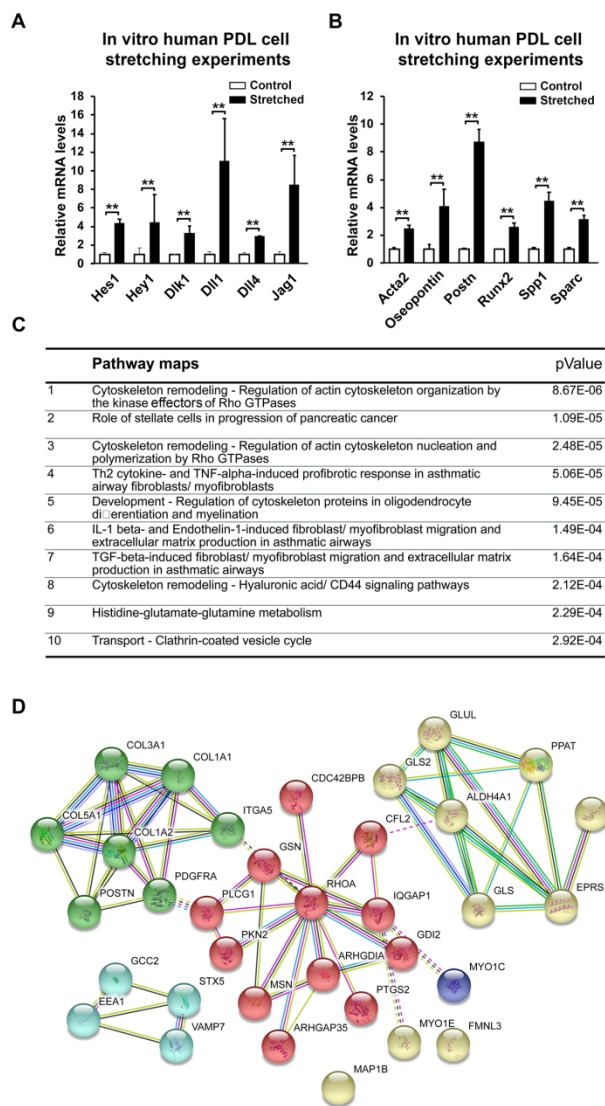


Figure 4

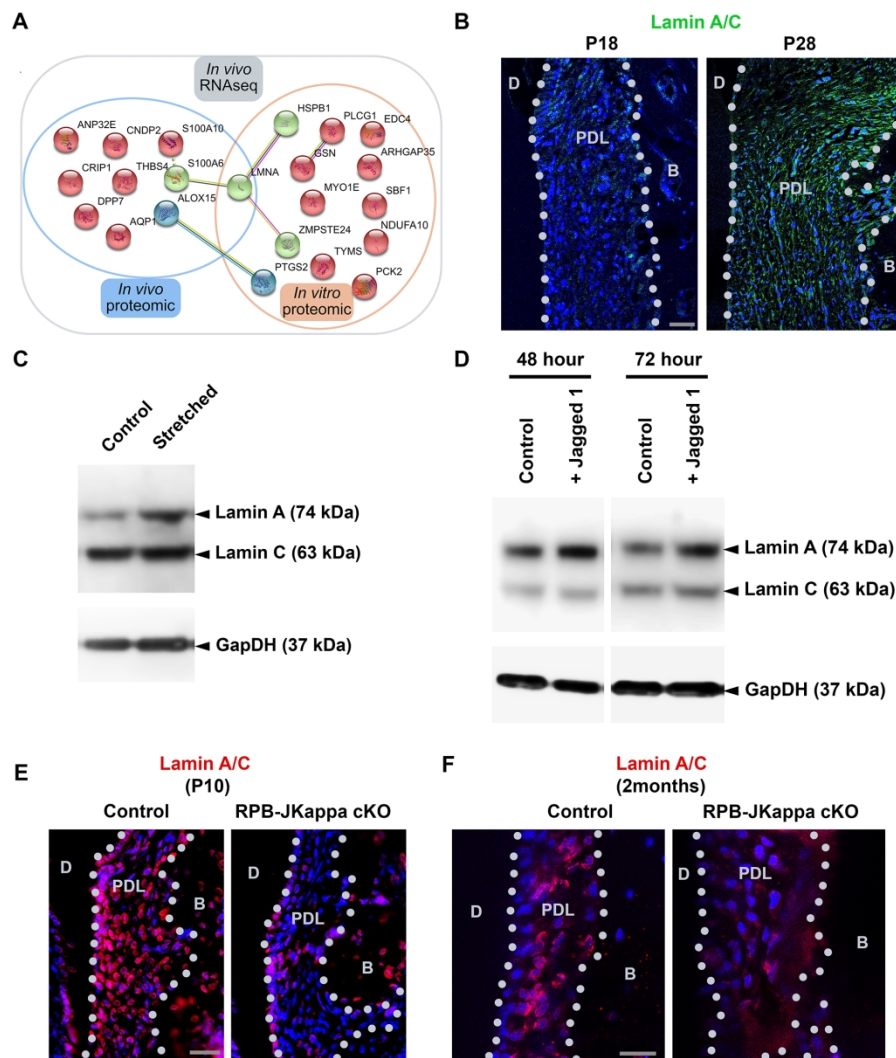


Figure 5

176x227mm (300 x 300 DPI)

1
2
3
4
5
6 **Notch coordinates periodontal ligament maturation through regulating Lamin A**

7
8
9
10
11 Balazs Jozsef Denes¹, Chloe Bolton², Charlotte Sara Illsley², Wai Ling Kok², Jemma Victoria
12
13 Walker², Ansgar Poetsch³, Christopher Tredwin², Stavros Kiliaridis¹, Bing Hu^{2*}

14
15
16
17 **Appendix files and legends**

18
19
20
21 **Appendix Figure 1**

22
23 A: Additional micro-CT analysis on P18 and P28 rat root.

24
25 B: Additional process network analysis on the RNAseq results illustrated in Figure 1.

26
27 Bar: 100µm

28
29
30 **Appendix Figure 2**

31
32 A: Periostin expression analysis at postnatal day 4 (P4) in the control and RBP-Jkappa cKO mice.

33
34 B: The stretching device system used in this study.

35
36 Bar: 20µm

37
38 **Appendix Figure 3**

39
40 Summarisation of the findings of study and perspectives.

41
42 **Appendix Table 1**

43
44 The RNAseq summary of the study.

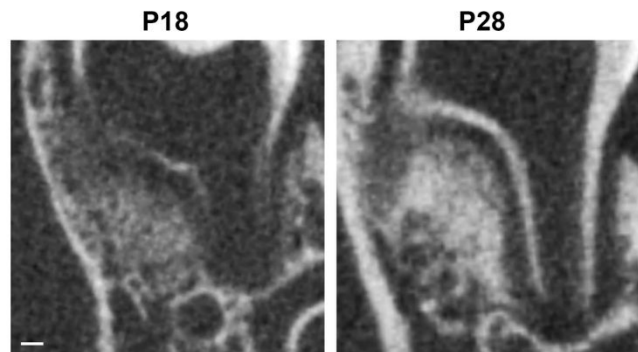
45
46 **Appendix Table 2**

1
2 The original proteomic analysis data of stretched PDL cells showed in Figure 4.
3
4
5
6

7 **Appendix Table 3**

8 The antibodies, primers and protein used in the study.
9
10
11
12
13
14
15

16 **A**

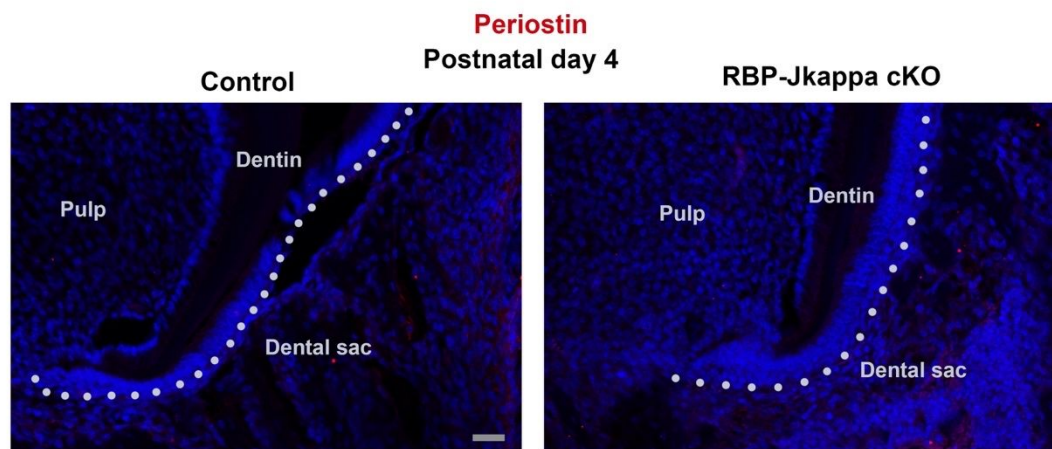


35 **B**

Process networks	pValue
1 Development - Neurogenesis - Axonal guidance	2.80E-04
2 Development - Ossification and bone remodeling	3.14E-04
3 Muscle contraction	3.69E-04
4 Signal Transduction - TGF-beta, GDF and Activin signaling	5.06E-04
5 Cell adhesion - Cell junctions	5.47E-04
6 Cell cycle - G1-S Growth factor regulation	7.53E-04
7 Signal transduction - NOTCH signaling	8.64E-04
8 Inflammation - IFN-gamma signaling	9.05E-04
9 Development - Blood vessel morphogenesis	9.24E-04
10 Proliferation - Positive regulation cell proliferation	9.86E-04

58 **Appendix Figure 1**

A



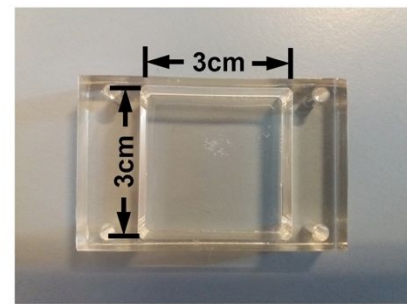
B



Stretching unit

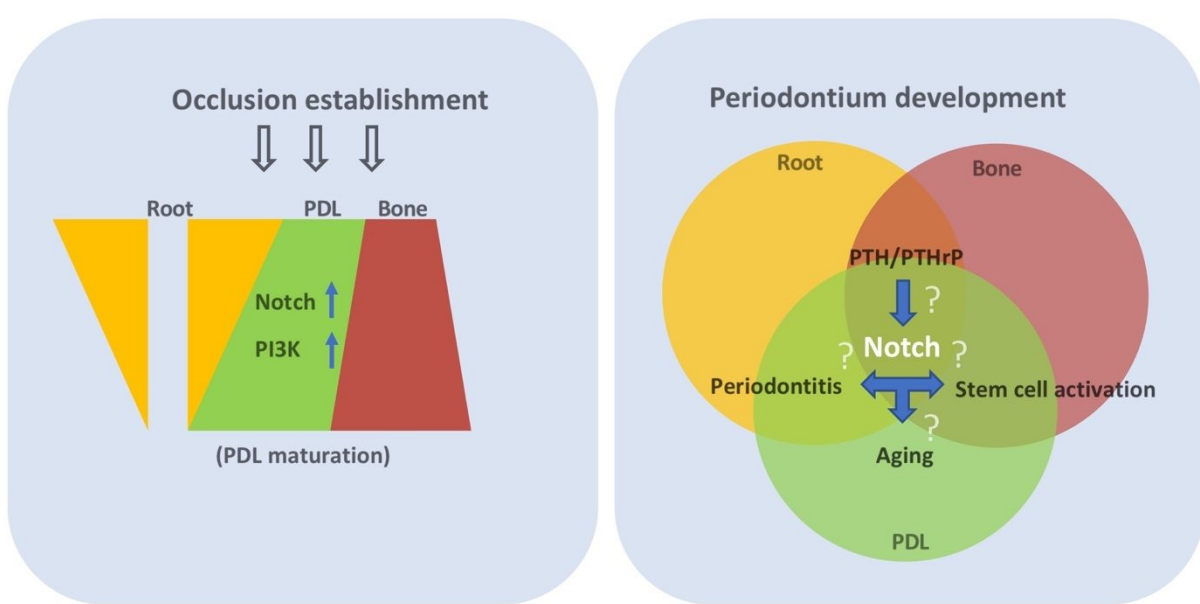
Controlling unit

C



Stretching chamber

Appendix Figure 2



Appendix Figure 3

Appendix Table 1

Summary of the fold changes of the genes up and down regulated comparing P28 with P18 PDL based on the RNAseq analysis results as showed in Figure 1D. The genes inside the category of “Cell” has been shown as below.

<i>A4galt</i>	56.2	0.012
<i>Aak1</i>	-6.2	0.046
<i>Aatf</i>	-3.0	0.001
<i>Abca2</i>	4.4	0.001
<i>Abca4</i>	-27.3	0.034
<i>Abca7</i>	5.6	0.036
<i>Abcc2</i>	-29.1	0.037
<i>Abcc5</i>	2.9	0.006
<i>Abcd3</i>	2.5	0.023
<i>Abce1</i>	-2.0	0.001
<i>Abi1</i>	1.7	0.008
<i>Abi3</i>	2.6	0.005
<i>Abt1</i>	1.5	0.046
<i>Acads</i>	1.6	0.038
<i>Acbd3</i>	2.1	0.032
<i>Acer1</i>	60.2	0.042
<i>Ache</i>	-10.8	0.013
<i>Ache</i>	-10.8	0.013
<i>Ackr2</i>	840.3	0.003
<i>Ackr3</i>	2.7	0.006
<i>Acot11</i>	-122.2	0.039
<i>Acox1</i>	-5.4	0.016
<i>Acp5</i>	12.7	0.001
<i>Acsbg1</i>	77.1	0.038
<i>Acta2</i>	-4.2	0.004
<i>Actr10</i>	-1.6	0.022
<i>Actr3</i>	-1.9	0.017
<i>Acvr1b</i>	24.5	0.044
<i>Adam19</i>	-1.8	0.044
<i>Adamts15</i>	32.3	0.036
<i>Adcy10</i>	89.7	0.015
<i>Adcy6</i>	2.4	0.029
<i>Adcyap1r1</i>	23.1	0.022
<i>Adh4</i>	16.2	0.046
<i>Adh5</i>	-1.5	0.020
<i>Adh6a</i>	-126.0	0.020
<i>Adh7</i>	1517.8	0.003
<i>Adm</i>	-10.4	0.000
<i>Adpgk</i>	-1.6	0.016

1	<i>Adra1b</i>	28.5	0.032
2	<i>Adrb1</i>	-59.2	0.048
3	<i>Adsl</i>	-1.9	0.003
4	<i>Afg3l2</i>	-1.7	0.048
5	<i>Aga</i>	1.7	0.009
6	<i>Agpat4</i>	-2.3	0.002
7	<i>Agps</i>	-2.9	0.042
8	<i>Ahnak</i>	2.2	0.032
9	<i>Aif1l</i>	-8.4	0.016
10	<i>Ak1</i>	-1.9	0.015
11	<i>Akap12</i>	2.2	0.018
12	<i>Akap17a</i>	2.6	0.021
13	<i>Akap5</i>	-158.1	0.017
14	<i>Akap8l</i>	2.4	0.001
15	<i>Akip1</i>	1.9	0.013
16	<i>Alad</i>	-1.8	0.045
17	<i>Alas2</i>	-5.7	0.012
18	<i>Aldh1a3</i>	-73.2	0.017
19	<i>Aldh1b1</i>	-159.0	0.002
20	<i>Aldh1l1</i>	-9.6	0.031
21	<i>Aldh6a1</i>	-1.8	0.013
22	<i>Alg11</i>	-3.1	0.000
23	<i>Alg2</i>	-2.6	0.004
24	<i>Alk</i>	339.8	0.006
25	<i>Alox15</i>	-11.1	0.001
26	<i>Als2</i>	-11.3	0.032
27	<i>Amelx</i>	-88.0	0.006
28	<i>Amigo1</i>	-147.1	0.025
29	<i>Ampd1</i>	60.5	0.011
30	<i>Amph</i>	-19.5	0.036
31	<i>Anapc1</i>	-1.7	0.033
32	<i>Anapc5</i>	-1.6	0.001
33	<i>Angptl6</i>	49.7	0.023
34	<i>Ankhd1</i>	2.1	0.011
35	<i>Ankrd13a</i>	-1.8	0.010
36	<i>Ankrd23</i>	22.9	0.036
37	<i>Anp32e</i>	-2.7	0.000
38	<i>Aox3</i>	31.0	0.032
39	<i>Ap1s2</i>	-1.7	0.026
40	<i>Ap2m1</i>	-1.7	0.003
41	<i>Aph1a</i>	-2.3	0.001
42	<i>Api5</i>	-1.7	0.004
43	<i>Apoc3</i>	55.0	0.011
44	<i>Aqp1</i>	2.7	0.015
45	<i>Aqp3</i>	211.9	0.001
46	<i>Aqp4</i>	1752.4	0.001

1	<i>Ar</i>	20.5	0.005
2	<i>Ar</i>	20.5	0.005
3	<i>Ar</i>	20.5	0.005
4	<i>Ar</i>	20.5	0.005
5	<i>Arcn1</i>	-1.9	0.001
6	<i>Arf1</i>	-1.8	0.021
7	<i>Arf2</i>	-1.9	0.017
8	<i>Arf4</i>	-1.5	0.004
9	<i>Arfip1</i>	-2.6	0.007
10	<i>Arfip2</i>	2.3	0.003
11	<i>Arg2</i>	5.8	0.000
12	<i>Arglu1</i>	2.0	0.028
13	<i>Arhgap35</i>	1.9	0.047
14	<i>Arhgap4</i>	-4.8	0.027
15	<i>Arhgef18</i>	-1.9	0.037
16	<i>Arhgef25</i>	-1.8	0.013
17	<i>Arhgef7</i>	-1.7	0.037
18	<i>Arl1</i>	-2.6	0.001
19	<i>Arl3</i>	1.6	0.015
20	<i>Arl6ip1</i>	-1.6	0.050
21	<i>Arntl</i>	2.3	0.025
22	<i>Arntl2</i>	-85.0	0.036
23	<i>Arrdc1</i>	1.6	0.009
24	<i>Arsi</i>	7.2	0.019
25	<i>Asgr2</i>	178.3	0.002
26	<i>Ash1l</i>	2.0	0.039
27	<i>Asic1</i>	79.2	0.023
28	<i>Asip</i>	71.8	0.027
29	<i>Atad1</i>	-2.0	0.021
30	<i>Ate1</i>	1.9	0.016
31	<i>Atf4</i>	1.6	0.012
32	<i>Atic</i>	-2.8	0.000
33	<i>Atl2</i>	-4.1	0.031
34	<i>Atoh8</i>	3.6	0.001
35	<i>Atp1a3</i>	-52.7	0.032
36	<i>Atp2a2</i>	-1.6	0.010
37	<i>Atp2b2</i>	98.2	0.013
38	<i>Atp2b3</i>	36.5	0.049
39	<i>Atp2b4</i>	1.9	0.038
40	<i>Atp5e</i>	2.0	0.030
41	<i>Atp5i</i>	1.7	0.039
42	<i>Atp5j2</i>	1.7	0.029
43	<i>Atp6v0b</i>	2.4	0.001
44	<i>Atp6v1e1</i>	1.7	0.005
45	<i>Atp6v1e2</i>	164.2	0.017
46	<i>Atp6v1f</i>	1.8	0.001

1	<i>Atxn10</i>	-2.2	0.000
2	<i>Avil</i>	417.1	0.000
3	<i>Avp</i>	183.0	0.008
4	<i>Azin2</i>	5.5	0.028
5	<i>B2m</i>	2.0	0.002
6	<i>B3galnt1</i>	-1.6	0.040
7	<i>B3galt1</i>	-264.1	0.037
8	<i>B3galt2</i>	-43.4	0.012
9	<i>B3galt6</i>	-3.0	0.018
10	<i>B3gat3</i>	1.9	0.001
11	<i>B4galnt4</i>	-13.4	0.047
12	<i>B4galt2</i>	-1.6	0.014
13	<i>B4galt6</i>	1.9	0.008
14	<i>B9d2</i>	1.8	0.013
15	<i>Bag3</i>	1.8	0.042
16	<i>Bag4</i>	-4.3	0.031
17	<i>Batf</i>	3.3	0.017
18	<i>Bbs2</i>	-2.0	0.043
19	<i>Bche</i>	-122.2	0.031
20	<i>Bckdhb</i>	-1.9	0.003
21	<i>Bcl2l15</i>	42.5	0.050
22	<i>Bcl6</i>	4.9	0.002
23	<i>Bcorl1</i>	2.4	0.034
24	<i>Bglap</i>	4.6	0.003
25	<i>Blk</i>	-17.9	0.002
26	<i>Bloc1s1</i>	1.6	0.037
27	<i>Blzf1</i>	-2.2	0.036
28	<i>Bmi1</i>	-7.3	0.013
29	<i>Bmpr1a</i>	-3.8	0.006
30	<i>Bmx</i>	-30.0	0.013
31	<i>Bod1</i>	1.6	0.028
32	<i>Brd9</i>	1.7	0.043
33	<i>Brf1</i>	-1.7	0.037
34	<i>Bri3</i>	2.4	0.009
35	<i>Brinp1</i>	-42.1	0.000
36	<i>Brinp2</i>	121.9	0.003
37	<i>Brms1l</i>	-4.0	0.006
38	<i>Btaf1</i>	1.7	0.046
39	<i>Btbd1</i>	-1.7	0.009
40	<i>Btbd6</i>	-1.7	0.010
41	<i>Btk</i>	-7.5	0.014
42	<i>Btnl2</i>	-63.2	0.022
43	<i>Btrc</i>	-2.8	0.015
44	<i>Bub1</i>	-2.7	0.013
45	<i>Bzw1</i>	-2.2	0.011
46	<i>Bzw2</i>	-2.0	0.001

1	<i>C1qa</i>	2.5	0.003
2	<i>C1qb</i>	1.9	0.041
3	<i>C1qc</i>	1.9	0.042
4	<i>Cacna1c</i>	-4.9	0.004
5	<i>Cacna2d4</i>	30.2	0.045
6	<i>Cacnb4</i>	74.6	0.018
7	<i>Cacng6</i>	-137.5	0.026
8	<i>Cadm1</i>	4.0	0.003
9	<i>Calb1</i>	-39.7	0.008
10	<i>Calcb</i>	-65.3	0.023
11	<i>Calm3</i>	-1.5	0.037
12	<i>Camk1g</i>	146.8	0.018
13	<i>Camk2a</i>	-34.6	0.047
14	<i>Camk2d</i>	-4.3	0.031
15	<i>Capg</i>	2.9	0.001
16	<i>Capn12</i>	4.9	0.005
17	<i>Capn15</i>	2.6	0.026
18	<i>Capn3</i>	-348.3	0.001
19	<i>Caprin1</i>	-2.1	0.002
20	<i>Capza1</i>	-1.9	0.002
21	<i>Capza2</i>	-1.6	0.014
22	<i>Carf</i>	15.0	0.025
23	<i>Carm1</i>	-2.1	0.017
24	<i>Casp1</i>	-4.0	0.017
25	<i>Casp4</i>	3.4	0.006
26	<i>Casp7</i>	-3.6	0.008
27	<i>Casp8</i>	-11.9	0.000
28	<i>Cav3</i>	72.1	0.044
29	<i>Cbll1</i>	1.9	0.003
30	<i>Cbx7</i>	7.3	0.049
31	<i>Ccar1</i>	1.7	0.035
32	<i>Ccdc22</i>	3.9	0.024
33	<i>Ccdc67</i>	-170.7	0.012
34	<i>Ccdc69</i>	-20.1	0.032
35	<i>Cchcr1</i>	1.8	0.020
36	<i>Ccl12</i>	112.4	0.015
37	<i>Ccl21</i>	258.3	0.014
38	<i>Ccna2</i>	-3.1	0.006
39	<i>Ccnb1</i>	-2.1	0.026
40	<i>Ccnb1ip1</i>	427.6	0.003
41	<i>Ccnd1</i>	2.1	0.025
42	<i>Ccndbp1</i>	1.9	0.004
43	<i>Ccnh</i>	-1.7	0.015
44	<i>Ccny</i>	-1.9	0.042
45	<i>Ccr7</i>	44.0	0.046
46	<i>Cct6a</i>	-1.6	0.011

1	<i>Cd164</i>	-1.8	0.001
2	<i>Cd177</i>	-22.0	0.027
3	<i>Cd19</i>	-64.0	0.004
4	<i>Cd22</i>	-97.8	0.002
5	<i>Cd244</i>	-34.9	0.016
6	<i>Cd320</i>	1.8	0.008
7	<i>Cd36</i>	-10.9	0.017
8	<i>Cd38</i>	-22.3	0.027
9	<i>Cd3g</i>	-10.1	0.032
10	<i>Cd44</i>	1.9	0.029
11	<i>Cd5</i>	92.0	0.023
12	<i>Cd55</i>	17.0	0.009
13	<i>Cd68</i>	3.0	0.013
14	<i>Cd69</i>	-569.3	0.003
15	<i>Cd79b</i>	-6.2	0.017
16	<i>Cd9</i>	2.3	0.000
17	<i>Cd99</i>	2.0	0.014
18	<i>Cdc123</i>	-1.7	0.005
19	<i>Cdc14a</i>	3.2	0.013
20	<i>Cdc16</i>	-2.2	0.000
21	<i>Cdc23</i>	-2.0	0.011
22	<i>Cdc26</i>	-2.7	0.000
23	<i>Cdc34</i>	1.7	0.026
24	<i>Cdc40</i>	-1.8	0.028
25	<i>Cdc6</i>	-4.8	0.015
26	<i>Cdca7</i>	-3.2	0.011
27	<i>Cdh1</i>	8.6	0.046
28	<i>Cdh13</i>	2.5	0.002
29	<i>Cdh17</i>	62.4	0.004
30	<i>Cdh2</i>	2.9	0.031
31	<i>Cdk2</i>	-2.1	0.047
32	<i>Cdk2ap2</i>	1.9	0.001
33	<i>Cdk5</i>	2.3	0.001
34	<i>Cdkn1a</i>	5.1	0.004
35	<i>Cdkn2a</i>	-71.7	0.035
36	<i>Cdkn2aip,Carf</i>	#N/A	#N/A
37	<i>Cdnf</i>	273.1	0.012
38	<i>Cdv3</i>	2.1	0.020
39	<i>Cebpd</i>	-1.8	0.029
40	<i>Cers3</i>	67.1	0.031
41	<i>Cfap126</i>	-129.8	0.019
42	<i>Cgnl1</i>	7.2	0.001
43	<i>Chchd10</i>	5.9	0.041
44	<i>Chi3l1</i>	-17.2	0.006
45	<i>Chp1</i>	-2.0	0.036
46	<i>Chpf2</i>	-1.7	0.016

1	<i>Chrna4</i>	-12.6	0.022
2	<i>Chrb1</i>	53.6	0.011
3	<i>Chst11</i>	11.2	0.039
4	<i>Chst12</i>	-1.7	0.035
5	<i>Chuk</i>	-2.3	0.011
6	<i>Cidea</i>	-247.0	0.012
7	<i>Cideb</i>	-27.2	0.032
8	<i>Cited1</i>	-39.0	0.035
9	<i>Cited2</i>	1.9	0.011
10	<i>Ckb</i>	2.1	0.024
11	<i>Cks2</i>	1.8	0.037
12	<i>Clca5</i>	155.2	0.008
13	<i>Clcn3</i>	-3.8	0.031
14	<i>Cldn10</i>	-443.2	0.001
15	<i>Cldn20</i>	-229.9	0.009
16	<i>Cldnd1</i>	-2.0	0.000
17	<i>Clip4</i>	24.3	0.048
18	<i>Clk1</i>	2.7	0.001
19	<i>Cln3</i>	2.9	0.013
20	<i>Cln8</i>	-2.8	0.011
21	<i>Clock</i>	2.6	0.030
22	<i>Clstrn1</i>	1.7	0.049
23	<i>Clstrn3</i>	424.9	0.001
24	<i>Clu</i>	-1.9	0.018
25	<i>Clvs1</i>	1.9	0.042
26	<i>Clvs2</i>	-76.4	0.041
27	<i>Cmc1</i>	2.1	0.006
28	<i>Cmpk1</i>	-1.7	0.001
29	<i>Cndp2</i>	-2.7	0.002
30	<i>Cnep1r1</i>	-2.2	0.026
31	<i>Cnih2</i>	-2.8	0.018
32	<i>Cnn3</i>	-1.6	0.016
33	<i>Cnot10</i>	2.1	0.003
34	<i>Cnp</i>	-1.8	0.016
35	<i>Cnp</i>	-1.8	0.016
36	<i>Cnrip1</i>	-1.7	0.032
37	<i>Cntf</i>	25.6	0.000
38	<i>Cntn1</i>	115.3	0.009
39	<i>Cntn6</i>	361.2	0.003
40	<i>Cntnap4</i>	1391.6	0.001
41	<i>Coa4</i>	2.0	0.007
42	<i>Coasy</i>	1.9	0.039
43	<i>Cog4</i>	-1.5	0.021
44	<i>Cog6</i>	-4.5	0.041
45	<i>Cog7</i>	-2.2	0.017
46	<i>Col26a1</i>	-3.6	0.017

1	<i>Col4a3bp</i>	3.3	0.028
2	<i>Col6a2</i>	2.0	0.007
3	<i>Comm4d</i>	1.9	0.003
4	<i>Copg1</i>	-2.1	0.022
5	<i>Coprs</i>	1.9	0.014
6	<i>Cops4</i>	-2.1	0.001
7	<i>Copz1</i>	-1.5	0.004
8	<i>Coq10b</i>	-2.1	0.028
9	<i>Coro1a</i>	-3.0	0.017
10	<i>Coro2a</i>	144.1	0.004
11	<i>Cotl1</i>	-1.7	0.021
12	<i>Cox17</i>	1.9	0.012
13	<i>Cox20</i>	1.7	0.029
14	<i>Cox7b</i>	2.0	0.013
15	<i>Cpeb1</i>	276.3	0.015
16	<i>Cpne9</i>	33.9	0.026
17	<i>Cpq</i>	1.6	0.032
18	<i>Cpsf4</i>	-2.1	0.038
19	<i>Cpt1c</i>	3.3	0.037
20	<i>Cr2</i>	-201.2	0.009
21	<i>Creb3l4</i>	186.5	0.009
22	<i>Crebbp</i>	1.7	0.049
23	<i>Crip1</i>	2.5	0.002
24	<i>Crip2</i>	1.7	0.009
25	<i>Crlf3</i>	-4.8	0.003
26	<i>Crls1</i>	-2.0	0.023
27	<i>Crtac1</i>	49.4	0.020
28	<i>Cs</i>	-1.8	0.010
29	<i>Csf2ra</i>	3.7	0.000
30	<i>Csnk1d</i>	-1.6	0.003
31	<i>Cspg4</i>	2.8	0.012
32	<i>Csrp2</i>	-1.7	0.033
33	<i>Cst3</i>	2.9	0.000
34	<i>Cstb</i>	1.8	0.021
35	<i>Cstf1</i>	-2.7	0.000
36	<i>Cstf2</i>	-2.8	0.045
37	<i>Ctbs</i>	1.7	0.042
38	<i>Ctdsp1</i>	1.8	0.002
39	<i>Ctdspl2</i>	-2.4	0.024
40	<i>Ctif</i>	33.6	0.034
41	<i>Ctps1</i>	-2.5	0.000
42	<i>Ctrb1</i>	98.1	0.013
43	<i>Ctsc</i>	-2.7	0.008
44	<i>Ctsd</i>	1.7	0.001
45	<i>Ctse</i>	-26.6	0.000
46	<i>Ctsf</i>	1.7	0.021

1	<i>Ctsw</i>	-76.8	0.003
2	<i>Ctsz</i>	3.6	0.004
3	<i>Cuedc2</i>	1.6	0.029
4	<i>Cul1</i>	-2.9	0.000
5	<i>Cul2</i>	-1.8	0.049
6	<i>Cul3</i>	-1.6	0.018
7	<i>Cxcl1</i>	305.7	0.011
8	<i>Cxcl10</i>	136.2	0.021
9	<i>Cxcl14</i>	-2.0	0.044
10	<i>Cxcr2</i>	-43.8	0.035
11	<i>Cxcr3</i>	30.2	0.042
12	<i>Cxcr6</i>	-226.8	0.025
13	<i>Cyb5b</i>	-1.6	0.034
14	<i>Cyba</i>	1.7	0.018
15	<i>Cyfip2</i>	-7.9	0.002
16	<i>Cyp27a1</i>	9.7	0.038
17	<i>Cyp27b1</i>	163.4	0.019
18	<i>Cyp2j10</i>	220.6	0.001
19	<i>Cyp2r1</i>	45.8	0.022
20	<i>Cyp39a1</i>	283.3	0.005
21	<i>Cyp3a9</i>	92.3	0.031
22	<i>Cyp4b1</i>	206.1	0.008
23	<i>Cyp7b1</i>	-5.8	0.003
24	<i>Cysltr1</i>	-103.8	0.039
25	<i>Dab2</i>	-1.7	0.027
26	<i>Dab2ip</i>	1.9	0.016
27	<i>Dapk1</i>	2.0	0.023
28	<i>Dars</i>	-2.4	0.013
29	<i>Dbf4</i>	-3.8	0.039
30	<i>Dbn1</i>	-1.5	0.045
31	<i>Dcaf8</i>	-1.8	0.002
32	<i>Dcdc2</i>	93.5	0.031
33	<i>Dcps</i>	-2.6	0.008
34	<i>Dcxr</i>	2.2	0.010
35	<i>Ddx46</i>	1.6	0.027
36	<i>Ddx50</i>	-1.6	0.037
37	<i>Ddx58</i>	3.8	0.022
38	<i>Ddx59</i>	2.1	0.025
39	<i>Dffa</i>	2.2	0.005
40	<i>Dgkg</i>	-15.8	0.028
41	<i>Dgki</i>	298.6	0.000
42	<i>Dhcr24</i>	-35.7	0.002
43	<i>Dhps</i>	-2.1	0.002
44	<i>Dhrs7c</i>	145.1	0.018
45	<i>Dhx30</i>	2.1	0.006
46	<i>Dhx8</i>	-2.6	0.013

1	<i>Dkk1</i>	-98.4	0.045
2	<i>Dlgap4</i>	2.1	0.002
3	<i>Dll1</i>	7.2	0.031
4	<i>Dnaja3</i>	-1.8	0.043
5	<i>Dnajb13</i>	263.7	0.002
6	<i>Dnajb4</i>	-2.1	0.016
7	<i>Dnajb6</i>	-2.1	0.015
8	<i>Dnajc16</i>	-900.3	0.000
9	<i>Dnase1l1</i>	2.9	0.011
10	<i>Dnase1l3</i>	-299.8	0.002
11	<i>Dnase2</i>	1.9	0.001
12	<i>Dnase2b</i>	44.0	0.019
13	<i>Dnlz</i>	1.9	0.021
14	<i>Dnm3</i>	-3.3	0.043
15	<i>Dock8</i>	-4.2	0.028
16	<i>Dock9</i>	2.9	0.034
17	<i>Dpep1</i>	29.8	0.039
18	<i>Dpf1</i>	92.0	0.001
19	<i>Dph3</i>	1.6	0.033
20	<i>Dpp4</i>	-19.8	0.004
21	<i>Dpp7</i>	1.8	0.010
22	<i>Dpyd</i>	84.5	0.003
23	<i>Dpysl2</i>	2.1	0.018
24	<i>Dram2</i>	-1.9	0.026
25	<i>Drg1</i>	-2.3	0.006
26	<i>Dsc3</i>	91.8	0.005
27	<i>Dsg3</i>	21.5	0.038
28	<i>Duox1</i>	3.7	0.011
29	<i>Dusp10</i>	-2.6	0.048
30	<i>Dusp3</i>	1.9	0.005
31	<i>Dusp4</i>	-33.4	0.038
32	<i>Dvl1</i>	2.1	0.012
33	<i>Dym</i>	-2.0	0.011
34	<i>Dync1i2</i>	1.5	0.047
35	<i>Dyrk2</i>	2.0	0.009
36	<i>Eaf2</i>	-36.5	0.041
37	<i>Edar</i>	-74.6	0.045
38	<i>Edc4</i>	2.1	0.003
39	<i>Eef1a1</i>	-1.9	0.018
40	<i>Eef1e1</i>	-2.1	0.003
41	<i>Efemp1</i>	5.1	0.037
42	<i>Egf</i>	22.1	0.036
43	<i>Egfl7</i>	1.9	0.012
44	<i>Egr2</i>	653.0	0.001
45	<i>Ehf</i>	187.0	0.020
46	<i>Ehmt1</i>	-5.3	0.001

1	<i>Ei24</i>	-2.2	0.000
2	<i>Eif2b1</i>	-1.6	0.011
3	<i>Eif2b3</i>	-2.5	0.003
4	<i>Eif2s1</i>	-1.6	0.018
5	<i>Eif4a1</i>	-1.5	0.002
6	<i>Eif4e</i>	-1.6	0.025
7	<i>Elf1</i>	-2.8	0.016
8	<i>Elf4</i>	-8.8	0.042
9	<i>Elov14</i>	-6.4	0.012
10	<i>Elov15</i>	-3.4	0.045
11	<i>Emc4</i>	1.7	0.002
12	<i>Emd</i>	2.1	0.020
13	<i>Emid1</i>	-2.9	0.000
14	<i>Eml1</i>	-3.1	0.020
15	<i>Enc1</i>	-3.1	0.010
16	<i>Enoph1</i>	-2.0	0.028
17	<i>Enpp1</i>	-2.5	0.018
18	<i>Enpp2</i>	3.1	0.020
19	<i>Enpp6</i>	130.7	0.001
20	<i>Eogt</i>	-23.6	0.015
21	<i>Epc1</i>	2.5	0.046
22	<i>Epha1</i>	233.9	0.003
23	<i>Epha2</i>	2.1	0.009
24	<i>Erh</i>	-1.6	0.001
25	<i>Espn</i>	30.6	0.008
26	<i>Esrp1</i>	73.2	0.017
27	<i>Esrp2</i>	130.5	0.025
28	<i>Etf1</i>	-1.5	0.030
29	<i>Etv1</i>	3.9	0.032
30	<i>Eva1a</i>	-1.8	0.027
31	<i>Evpl</i>	203.0	0.010
32	<i>Exoc6b</i>	-3.4	0.003
33	<i>Ezh1</i>	3.7	0.009
34	<i>F11r</i>	-1.8	0.047
35	<i>F12</i>	-154.6	0.010
36	<i>F2r</i>	-2.8	0.001
37	<i>Fa2h</i>	25.3	0.037
38	<i>Fabp5</i>	2.7	0.015
39	<i>Fah</i>	5.6	0.007
40	<i>Fam118b</i>	-2.1	0.045
41	<i>Fam126a</i>	-22.4	0.000
42	<i>Fam126b</i>	4.2	0.035
43	<i>Fam161a</i>	-82.9	0.016
44	<i>Fam172a</i>	-2.0	0.025
45	<i>Fam20c</i>	3.1	0.003
46	<i>Fam26e</i>	-15.4	0.041

1	<i>Fam26f</i>	25.2	0.039
2	<i>Fam46c</i>	-2.4	0.032
3	<i>Fam65a</i>	1.9	0.010
4	<i>Fam96b</i>	1.7	0.010
5	<i>Fam98c</i>	1.7	0.021
6	<i>Fanca</i>	4.9	0.003
7	<i>Farsb</i>	-3.9	0.000
8	<i>Fasn</i>	1.7	0.039
9	<i>Fat1</i>	2.3	0.036
10	<i>Fbxl4</i>	-4.1	0.024
11	<i>Fbxl5</i>	-1.7	0.042
12	<i>Fbxo2</i>	204.6	0.026
13	<i>Fbxo39</i>	42.3	0.042
14	<i>Fbxo44</i>	214.6	0.016
15	<i>Fbxo7</i>	-2.0	0.033
16	<i>Fcmr</i>	-5.2	0.020
17	<i>Fcnb</i>	-13.2	0.012
18	<i>Fcrla</i>	-6.4	0.049
19	<i>Fdx1</i>	1.6	0.010
20	<i>Fem1a</i>	1.8	0.003
21	<i>Fermt1</i>	5.8	0.036
22	<i>Fgd4</i>	37.1	0.009
23	<i>Fgf9</i>	57.2	0.022
24	<i>Fgfbp1</i>	1831.0	0.002
25	<i>Fgfrl1</i>	3.0	0.007
26	<i>Fhl2</i>	-2.3	0.015
27	<i>Fhod1</i>	4.1	0.006
28	<i>Fibp</i>	1.5	0.005
29	<i>Flrt1</i>	123.3	0.010
30	<i>Flrt3</i>	-3.5	0.025
31	<i>Flt3</i>	27.8	0.023
32	<i>Fmr1</i>	2.1	0.006
33	<i>Fndc3a</i>	3.3	0.002
34	<i>Fnip1</i>	2.7	0.008
35	<i>Fnip2</i>	23.1	0.007
36	<i>Folh1</i>	-151.6	0.044
37	<i>Folr2</i>	3.5	0.010
38	<i>Foxi3</i>	45.4	0.037
39	<i>Foxj1</i>	109.3	0.021
40	<i>Foxk1</i>	-3.7	0.040
41	<i>Foxo3</i>	2.2	0.015
42	<i>Foxo4</i>	6.1	0.024
43	<i>Fpr1</i>	-282.3	0.003
44	<i>Frmd3</i>	-143.3	0.027
45	<i>Fscn3</i>	531.0	0.006
46	<i>Fsd1</i>	-242.3	0.011

1	<i>Fto</i>	-5.3	0.004
2	<i>Fundc2</i>	1.6	0.015
3	<i>Furin</i>	-2.0	0.000
4	<i>Fut11</i>	-2.8	0.037
5	<i>Fut7</i>	215.2	0.003
6	<i>Fut8</i>	-5.7	0.000
7	<i>Fxyd1</i>	1.8	0.038
8	<i>Fxyd2</i>	6.8	0.000
9	<i>Fxyd3</i>	5.4	0.034
10	<i>G3bp1</i>	-1.9	0.002
11	<i>G3bp2</i>	-4.0	0.024
12	<i>Gabarapl1</i>	1.8	0.003
13	<i>Gabbr1</i>	2.9	0.007
14	<i>Gabbr2</i>	533.6	0.004
15	<i>Gabrd</i>	39.1	0.019
16	<i>Gadd45g</i>	1.8	0.021
17	<i>Gale</i>	2.5	0.017
18	<i>Galm</i>	2.2	0.037
19	<i>Galnt1</i>	-3.2	0.009
20	<i>Galnt10</i>	-4.4	0.002
21	<i>Galt</i>	1.6	0.050
22	<i>Gatad2b</i>	2.9	0.019
23	<i>Gatm</i>	-2.7	0.009
24	<i>Gba2</i>	1.8	0.034
25	<i>Gc</i>	-122.8	0.017
26	<i>Gcgr</i>	27.5	0.025
27	<i>Gcn1l1</i>	1.8	0.040
28	<i>Gfi1</i>	-52.5	0.017
29	<i>Ggps1</i>	-2.7	0.014
30	<i>Ghr</i>	-2.0	0.005
31	<i>Ghrl</i>	19.6	0.042
32	<i>Gimap4</i>	2.6	0.024
33	<i>Gimap7</i>	-12.6	0.028
34	<i>Gjb2</i>	43.7	0.022
35	<i>Gjb3</i>	131.2	0.027
36	<i>Gjc1</i>	-2.6	0.004
37	<i>Gldn</i>	23.6	0.035
38	<i>Glrb</i>	-70.6	0.008
39	<i>Glxr</i>	-2.4	0.001
40	<i>Gls</i>	1.8	0.018
41	<i>Gls</i>	1.8	0.018
42	<i>Gmnn</i>	-2.6	0.009
43	<i>Gmpa</i>	1.8	0.006
44	<i>Gmppb</i>	-2.8	0.000
45	<i>Gmps</i>	-1.7	0.029
46	<i>Gnai3</i>	-1.5	0.012

1	<i>Gnal</i>	-1.7	0.018
2	<i>Gnb1</i>	-1.6	0.014
3	<i>Gngt2</i>	2.3	0.013
4	<i>Gnl2</i>	-2.5	0.005
5	<i>Gnl3</i>	-1.5	0.019
6	<i>Gnpda2</i>	-2.9	0.028
7	<i>Gnpnat1</i>	-2.2	0.003
8	<i>Golga1</i>	3.8	0.003
9	<i>Golga7</i>	-1.9	0.026
10	<i>Golt1b</i>	-1.7	0.040
11	<i>Gorasp2</i>	-1.5	0.043
12	<i>Gpc1</i>	1.7	0.030
13	<i>Gpc3</i>	-10.5	0.000
14	<i>Gpc4</i>	-1.7	0.043
15	<i>Gpcpd1</i>	-2.6	0.002
16	<i>Gpnmb</i>	3.1	0.033
17	<i>Gpr174</i>	58.6	0.010
18	<i>Gprc5a</i>	65.2	0.021
19	<i>Gpsm2</i>	-2.5	0.001
20	<i>Grb10</i>	-1.8	0.029
21	<i>Grik4</i>	108.0	0.005
22	<i>Grin2c</i>	-84.4	0.049
23	<i>Grm7</i>	64.4	0.029
24	<i>Grsf1</i>	-1.8	0.001
25	<i>Gsn</i>	2.1	0.001
26	<i>Gsr</i>	-2.1	0.014
27	<i>Gstk1</i>	2.2	0.020
28	<i>Gstm5</i>	-1.8	0.012
29	<i>Gtpbp2</i>	3.1	0.000
30	<i>Haa0</i>	-139.1	0.014
31	<i>Hadh</i>	-2.5	0.044
32	<i>Hat1</i>	-2.6	0.000
33	<i>Havcr2</i>	-327.5	0.027
34	<i>Hbp1</i>	-2.1	0.002
35	<i>Hcfc1r1</i>	1.7	0.017
36	<i>Hdac1</i>	-1.6	0.018
37	<i>Hdac10</i>	2.5	0.036
38	<i>Hdac2</i>	-1.8	0.000
39	<i>Hexa</i>	1.7	0.005
40	<i>Hexim2</i>	-2.2	0.016
41	<i>Hgfac</i>	265.0	0.011
42	<i>Hibadh</i>	-2.2	0.013
43	<i>Hif1a</i>	-1.9	0.002
44	<i>Higd1a</i>	1.6	0.031
45	<i>Hint2</i>	2.1	0.007
46	<i>Hip1</i>	2.0	0.014

1	<i>Hipk2</i>	3.7	0.031
2	<i>Hist1h2bh</i>	2.1	0.012
3	<i>Hist1h4m,Hist1h4b</i>	#N/A	#N/A
4	<i>Hivep1</i>	3.1	0.019
5	<i>Hivep3</i>	-4.9	0.028
6	<i>Hmgcl</i>	2.1	0.010
7	<i>Hmgn2</i>	-2.3	0.000
8	<i>Hnrnpa2b1</i>	-1.8	0.017
9	<i>Hnrnpdl</i>	-1.6	0.020
10	<i>Hnrnpf</i>	-1.8	0.030
11	<i>Hnrnph2</i>	-2.2	0.033
12	<i>Hnrnpu</i>	-1.5	0.002
13	<i>Hoxb4</i>	-27.5	0.042
14	<i>Hoxd4</i>	6.8	0.031
15	<i>Hoxd9</i>	31.9	0.044
16	<i>Hp</i>	-3.3	0.036
17	<i>Hpd</i>	-110.3	0.027
18	<i>Hras</i>	1.6	0.027
19	<i>Hrh1</i>	-260.9	0.025
20	<i>Hrh3</i>	-311.0	0.011
21	<i>Hrk</i>	66.4	0.032
22	<i>Hsd17b14</i>	97.6	0.023
23	<i>Hsd17b8</i>	2.4	0.001
24	<i>Hsdl2</i>	-1.9	0.045
25	<i>Hsf2</i>	-2.2	0.028
26	<i>Hspa1l</i>	128.5	0.022
27	<i>Hspa5</i>	-1.7	0.002
28	<i>Hspb1</i>	4.6	0.000
29	<i>Hspf1</i>	2.1	0.013
30	<i>Htr1b</i>	-87.1	0.027
31	<i>Htr2b</i>	50.1	0.015
32	<i>Htr7</i>	-107.7	0.027
33	<i>Ica1</i>	2.9	0.024
34	<i>Icam4</i>	-322.7	0.009
35	<i>Icam5</i>	30.9	0.034
36	<i>Idh3a</i>	-1.9	0.012
37	<i>Ifi27</i>	1.9	0.013
38	<i>Ifi27l2b</i>	7.6	0.000
39	<i>Ifngr2</i>	1.7	0.014
40	<i>Ift57</i>	-1.8	0.004
41	<i>Igfp1</i>	1.9	0.030
42	<i>Igfbp6</i>	54.1	0.000
43	<i>Ikbip</i>	-2.7	0.002
44	<i>Il11</i>	83.2	0.026
45	<i>Il16</i>	-10.1	0.000
46	<i>Il1rl1</i>	-27.1	0.021

1	<i>Il3ra</i>	2.5	0.020
2	<i>Ilf2</i>	-1.8	0.017
3	<i>Ilf3</i>	1.6	0.033
4	<i>Impa1</i>	-2.2	0.001
5	<i>Ina</i>	-32.5	0.035
6	<i>Ing4</i>	1.6	0.007
7	<i>Inha</i>	6.7	0.009
8	<i>Inhba</i>	3.1	0.026
9	<i>Ino80</i>	2.5	0.039
10	<i>Insc</i>	-2.0	0.030
11	<i>Insig2</i>	1.9	0.029
12	<i>Insl3</i>	143.6	0.017
13	<i>Ip6k1</i>	-2.8	0.015
14	<i>Ireb2</i>	-2.6	0.041
15	<i>Irf3</i>	1.9	0.011
16	<i>Irgm</i>	4.3	0.012
17	<i>Irx2</i>	51.0	0.008
18	<i>Irx6</i>	198.9	0.005
19	<i>Isoc1</i>	-2.5	0.001
20	<i>Itch</i>	-3.9	0.027
21	<i>Itga10</i>	5.5	0.001
22	<i>Itga11</i>	-2.9	0.009
23	<i>Itga4</i>	-9.7	0.005
24	<i>Itga8</i>	28.9	0.021
25	<i>Itgae</i>	1.8	0.039
26	<i>Itgb1bp2</i>	66.9	0.017
27	<i>Itgb4</i>	3.1	0.009
28	<i>Itgb6</i>	142.4	0.013
29	<i>Itm2a</i>	-2.4	0.002
30	<i>Itpka</i>	300.2	0.010
31	<i>Itpkb</i>	-8.6	0.023
32	<i>Itsni</i>	-3.2	0.020
33	<i>Jade3</i>	-536.5	0.002
34	<i>Jmjd1c</i>	1.9	0.011
35	<i>Jmjd8</i>	1.7	0.006
36	<i>Junb</i>	1.9	0.010
37	<i>Kank1</i>	3.9	0.017
38	<i>Kars</i>	-1.6	0.007
39	<i>Kat7</i>	-1.8	0.049
40	<i>Kcna1</i>	149.8	0.018
41	<i>Kcna2</i>	-182.6	0.045
42	<i>Kcna3</i>	-92.5	0.043
43	<i>Kcnab3</i>	108.8	0.007
44	<i>Kcng1</i>	-338.6	0.005
45	<i>Kcnj12</i>	122.8	0.039
46	<i>Kcnj15</i>	93.7	0.021

1	<i>Kcnj9</i>	86.0	0.016
2	<i>Kcnmb4</i>	3.1	0.001
3	<i>Kcnq1</i>	126.4	0.021
4	<i>Kcnrg</i>	-178.6	0.005
5	<i>Kctd1</i>	1.9	0.033
6	<i>Kctd3</i>	-3.3	0.001
7	<i>Kdelc2</i>	-1.7	0.049
8	<i>Kdm1a</i>	-1.7	0.003
9	<i>Kdm4c</i>	-11.3	0.000
10	<i>Kdm8</i>	2.0	0.038
11	<i>Keap1</i>	1.8	0.007
12	<i>Kif19</i>	72.2	0.037
13	<i>Kif1c</i>	2.7	0.030
14	<i>Kif26b</i>	-4.6	0.030
15	<i>Kif27</i>	-91.5	0.016
16	<i>Kifc2</i>	15.4	0.039
17	<i>Kit</i>	-33.8	0.013
18	<i>Klf1</i>	-30.1	0.002
19	<i>Klf13</i>	1.9	0.004
20	<i>Klf16</i>	-2.1	0.004
21	<i>Klf3</i>	1.7	0.007
22	<i>Klf4</i>	6.5	0.000
23	<i>Klf5</i>	4.5	0.026
24	<i>Klhd10</i>	-3.3	0.040
25	<i>Klhd3</i>	-1.8	0.001
26	<i>Klh14</i>	-25.3	0.037
27	<i>Klh22</i>	-1.6	0.034
28	<i>Klh40</i>	209.8	0.026
29	<i>Klh41</i>	145.5	0.015
30	<i>Klh8</i>	2.1	0.034
31	<i>Klh9</i>	-1.7	0.011
32	<i>Klk4</i>	-2388.5	0.004
33	<i>Klk8</i>	115.4	0.021
34	<i>Klk8</i>	115.4	0.021
35	<i>Klrk1</i>	-114.8	0.025
36	<i>Kmt2e</i>	1.8	0.002
37	<i>Kpna1</i>	-2.5	0.047
38	<i>Kpnb1</i>	-2.4	0.010
39	<i>Krt10</i>	2.4	0.034
40	<i>Krt15</i>	366.7	0.013
41	<i>Krt17</i>	21.1	0.033
42	<i>Krt80</i>	611.8	0.008
43	<i>Ksr1</i>	-6.0	0.011
44	<i>L3mbtl2</i>	2.0	0.035
45	<i>Lamtor2</i>	1.7	0.011
46	<i>Lamtor4</i>	1.7	0.009

1	<i>Lanc12</i>	-4.1	0.036
2	<i>Laptm4b</i>	-2.0	0.000
3	<i>Larp6</i>	3.8	0.002
4	<i>Lbr</i>	-3.2	0.032
5	<i>Lbr</i>	-3.2	0.032
6	<i>Ldah</i>	-3.1	0.003
7	<i>Ldb2</i>	2.5	0.010
8	<i>Leprot</i>	1.7	0.004
9	<i>Lgals3</i>	5.3	0.000
10	<i>Lgals7</i>	165.8	0.002
11	<i>Lgr5</i>	390.4	0.014
12	<i>Lime1</i>	13.5	0.004
13	<i>Lims1</i>	-2.3	0.001
14	<i>Liph</i>	105.6	0.024
15	<i>Litaf</i>	1.8	0.003
16	<i>Lix1l</i>	2.2	0.006
17	<i>Llg1l</i>	-2.0	0.003
18	<i>Lmbr1l</i>	2.7	0.041
19	<i>Lmf2</i>	2.0	0.000
20	<i>Lmna</i>	1.5	0.033
21	<i>Lmnb1</i>	-3.1	0.017
22	<i>LOC100302465</i>	-164.2	0.023
23	<i>Lpar6</i>	-1.7	0.050
24	<i>Lpp</i>	2.3	0.030
25	<i>Lrfn4</i>	1.8	0.030
26	<i>Lrrc1</i>	-4.4	0.044
27	<i>Lrrc29</i>	255.4	0.001
28	<i>Lrrc46</i>	802.5	0.001
29	<i>Lrrc4b</i>	2.6	0.031
30	<i>Lrrc59</i>	-1.6	0.048
31	<i>Lrrn3</i>	-19.7	0.036
32	<i>LRRTM1</i>	-28.4	0.007
33	<i>Lsm14a</i>	-1.5	0.031
34	<i>Lsm8</i>	1.6	0.025
35	<i>Lss</i>	-10.1	0.001
36	<i>Lst1</i>	-5.0	0.010
37	<i>Lta4h</i>	-1.8	0.030
38	<i>Ltbp1</i>	2.8	0.001
39	<i>Ltv1</i>	-1.9	0.012
40	<i>Luc7l</i>	2.2	0.001
41	<i>Ly6d</i>	840.4	0.000
42	<i>Ly6g6f</i>	-78.6	0.028
43	<i>Lynx1</i>	835.0	0.020
44	<i>Lypd3</i>	12.4	0.022
45	<i>Lypla1</i>	-2.1	0.003
46	<i>Magt1</i>	-3.6	0.000

1	<i>Mal2</i>	113.9	0.010
2	<i>Mamdc4</i>	73.4	0.016
3	<i>Man1a1</i>	-3.6	0.027
4	<i>Maoa</i>	-2.4	0.033
5	<i>Map2</i>	-25.9	0.033
6	<i>Map2</i>	-25.9	0.033
7	<i>Map3k11</i>	2.1	0.040
8	<i>Map4k1</i>	-3.2	0.012
9	<i>Map4k4</i>	2.4	0.022
10	<i>Mapk11</i>	139.4	0.017
11	<i>Mapk13</i>	64.3	0.007
12	<i>Mapre1</i>	-1.6	0.009
13	<i>Mapt</i>	20.7	0.042
14	<i>Marc1</i>	4.3	0.036
15	<i>March2</i>	2.3	0.000
16	<i>March3</i>	-4.1	0.015
17	<i>March5</i>	-2.2	0.010
18	<i>March7</i>	-7.2	0.000
19	<i>Matk</i>	4.5	0.026
20	<i>Mbip</i>	-2.5	0.020
21	<i>Mcc</i>	21.3	0.027
22	<i>Mccc1</i>	-2.5	0.049
23	<i>Mccc2</i>	-1.9	0.048
24	<i>Mcf2d</i>	-1.9	0.001
25	<i>Mcl1</i>	-1.6	0.026
26	<i>Mcm10</i>	-43.8	0.000
27	<i>Mcm2</i>	-2.8	0.005
28	<i>Mcm4</i>	-2.1	0.010
29	<i>Mcm6</i>	-2.6	0.017
30	<i>Mcoln3</i>	75.4	0.014
31	<i>Mcpt2</i>	-421.7	0.003
32	<i>Mdfic</i>	1.7	0.043
33	<i>Mdk</i>	-1.7	0.031
34	<i>Me3</i>	131.8	0.003
35	<i>Mea1</i>	1.6	0.014
36	<i>Med13</i>	2.3	0.006
37	<i>Med15</i>	1.7	0.003
38	<i>Med19</i>	1.7	0.029
39	<i>Med20</i>	-2.0	0.009
40	<i>Med31</i>	1.8	0.002
41	<i>Mef2b</i>	-53.1	0.047
42	<i>Mei4</i>	-137.5	0.028
43	<i>Mest</i>	-6.6	0.000
44	<i>Mettl23</i>	1.8	0.030
45	<i>Mettl4</i>	-12.7	0.025
46	<i>Mfsd12</i>	-26.6	0.014

1	<i>Mgarp</i>	341.5	0.005
2	<i>Mgp</i>	2.2	0.034
3	<i>Mgrn1</i>	-2.8	0.006
4	<i>Mid1ip1</i>	2.3	0.023
5	<i>Mina</i>	-3.0	0.001
6	<i>Mios</i>	-2.9	0.001
7	<i>Mis12</i>	-2.5	0.022
8	<i>Mknk2</i>	-1.6	0.020
9	<i>Mlana</i>	35.3	0.001
10	<i>Mlph</i>	76.0	0.020
11	<i>Mmgt1</i>	-2.8	0.049
12	<i>Mmp23</i>	-1.8	0.038
13	<i>Mmp24</i>	2.2	0.019
14	<i>Mmp3</i>	107.3	0.012
15	<i>Mok</i>	4.7	0.036
16	<i>Morc1</i>	-58.8	0.038
17	<i>Morf4l2</i>	-1.7	0.001
18	<i>Mospd4</i>	146.2	0.013
19	<i>Mpc2</i>	1.9	0.008
20	<i>Mpg</i>	1.6	0.040
21	<i>Mpp6</i>	-1.9	0.015
22	<i>Mrip</i>	-1.5	0.015
23	<i>Mpv17l2</i>	1.7	0.022
24	<i>Mpzl2</i>	21.1	0.023
25	<i>Mrc1</i>	1.8	0.031
26	<i>Mri1</i>	2.8	0.004
27	<i>Mrpl14</i>	1.6	0.022
28	<i>Mrpl32</i>	1.7	0.009
29	<i>Mrpl54</i>	1.8	0.041
30	<i>mrpl9</i>	2.1	0.001
31	<i>Mrps2</i>	-2.0	0.026
32	<i>Mrps22</i>	1.8	0.049
33	<i>Mrps27</i>	-2.2	0.049
34	<i>Mrps30</i>	-1.8	0.025
35	<i>Ms4a1</i>	-12.6	0.014
36	<i>Ms4a2</i>	-40.1	0.014
37	<i>Msl1</i>	1.7	0.006
38	<i>Mst1r</i>	41.7	0.049
39	<i>Msto1</i>	2.2	0.047
40	<i>Mt1a</i>	7.5	0.000
41	<i>Mt3</i>	60.7	0.000
42	<i>Mt4</i>	1334.1	0.003
43	<i>Mta2</i>	-1.7	0.015
44	<i>Mterfd1</i>	-2.2	0.000
45	<i>Mtf2</i>	-1.6	0.041
46	<i>Mtmr2</i>	-1.8	0.048

1	<i>Mtmr7</i>	-52.9	0.020
2	<i>Mto1</i>	3.2	0.037
3	<i>Mtrr</i>	2.7	0.017
4	<i>Muc1</i>	233.8	0.004
5	<i>Muc20</i>	-445.1	0.007
6	<i>Mvb12a</i>	1.9	0.002
7	<i>Mx2</i>	229.4	0.010
8	<i>Mybl1</i>	80.7	0.010
9	<i>Myc</i>	-2.0	0.001
10	<i>Mycbp2</i>	2.1	0.028
11	<i>Myh10</i>	-1.6	0.043
12	<i>Myl1</i>	1233.0	0.003
13	<i>Mylpf</i>	6.6	0.043
14	<i>Myo1d</i>	3.0	0.001
15	<i>Myo1e</i>	2.6	0.043
16	<i>Myo7a</i>	30.1	0.045
17	<i>Myo9a</i>	3.3	0.006
18	<i>Myoc</i>	155.0	0.011
19	<i>Myof</i>	2.5	0.019
20	<i>Myom2</i>	706.7	0.004
21	<i>Mzb1</i>	-17.6	0.021
22	<i>N4bp2l2</i>	1.7	0.008
23	<i>Nadk2</i>	-3.7	0.010
24	<i>Nags</i>	82.2	0.006
25	<i>Ncaph2</i>	-2.0	0.012
26	<i>Ncbp1</i>	-1.9	0.003
27	<i>Ncf2</i>	-117.9	0.014
28	<i>Ncoa5</i>	-2.6	0.000
29	<i>Ndel1</i>	-1.6	0.033
30	<i>Ndfip2</i>	-1.9	0.004
31	<i>Ndufa10</i>	-1.7	0.004
32	<i>Ndufaf1</i>	-9.7	0.006
33	<i>Ndufs5</i>	2.3	0.003
34	<i>Nek6</i>	-4.0	0.000
35	<i>Neto2</i>	-5.7	0.046
36	<i>Neu3</i>	25.5	0.012
37	<i>Nfat5</i>	2.1	0.047
38	<i>Nfatc1</i>	1.7	0.017
39	<i>Nfil3</i>	-2.3	0.019
40	<i>Nfkbia</i>	1.5	0.002
41	<i>Nfkbiz</i>	6.4	0.011
42	<i>Nfx1</i>	-2.6	0.001
43	<i>Ngp</i>	-19.0	0.011
44	<i>Nin</i>	6.7	0.003
45	<i>Nkx2-3</i>	67.5	0.028
46	<i>Nkx6-3</i>	94.9	0.009

1	<i>Nmbr</i>	49.8	0.044
2	<i>Nmnat2</i>	70.0	0.026
3	<i>Nmur1</i>	-108.6	0.030
4	<i>Nnat</i>	4.5	0.000
5	<i>Nnt</i>	-1.5	0.017
6	<i>Nob1</i>	1.7	0.011
7	<i>Noc2l</i>	-3.1	0.001
8	<i>Nod2</i>	23.3	0.037
9	<i>Nol10</i>	-2.4	0.019
10	<i>Nop56</i>	-1.7	0.033
11	<i>Nop58</i>	-1.5	0.028
12	<i>Nos1</i>	41.0	0.035
13	<i>Nos2</i>	63.9	0.025
14	<i>Notch1</i>	2.1	0.011
15	<i>Notch4</i>	2.1	0.018
16	<i>Npas2</i>	5.5	0.010
17	<i>Npc1</i>	3.0	0.003
18	<i>Nphs1</i>	67.9	0.027
19	<i>Npr3</i>	-423.3	0.014
20	<i>Nptn</i>	1.6	0.005
21	<i>Npy4r</i>	-131.4	0.035
22	<i>Npy5r</i>	64.0	0.040
23	<i>Nr0b2</i>	416.4	0.002
24	<i>Nr1h2</i>	1.7	0.002
25	<i>Nr2c1</i>	-2.3	0.017
26	<i>Nr4a1</i>	2.4	0.047
27	<i>Nras</i>	-2.2	0.047
28	<i>Nrg1</i>	103.2	0.011
29	<i>Nrg1</i>	103.2	0.011
30	<i>Nrg2</i>	-8.5	0.043
31	<i>Nrp2</i>	-2.2	0.042
32	<i>Nrxn1</i>	-5.6	0.039
33	<i>Nsg1</i>	-1.9	0.022
34	<i>Nsmce4a</i>	-1.7	0.014
35	<i>Nsun2</i>	-2.3	0.001
36	<i>Nt5c1b</i>	-70.8	0.048
37	<i>Ntmt1</i>	1.6	0.005
38	<i>Ntn3</i>	-3.0	0.048
39	<i>Nuak2</i>	14.4	0.027
40	<i>Nudt17</i>	342.1	0.005
41	<i>Nufip1</i>	-2.1	0.013
42	<i>Numa1</i>	2.0	0.003
43	<i>Nup35</i>	-1.8	0.034
44	<i>Nup62</i>	-2.1	0.003
45	<i>Nup93</i>	-1.9	0.012
46	<i>Nupl1</i>	-5.9	0.004

1	<i>Nus1</i>	-1.8	0.010
2	<i>Oas3</i>	81.3	0.017
3	<i>Oat</i>	-1.6	0.001
4	<i>Ogdhl</i>	13.2	0.014
5	<i>Ogdhl,Ogdh</i>	#N/A	#N/A
6	<i>Ogfr</i>	1.7	0.004
7	<i>Olfm4</i>	-16.4	0.045
8	<i>Ormdl2</i>	2.1	0.001
9	<i>Ormdl3</i>	-1.9	0.044
10	<i>Ovol1</i>	120.7	0.009
11	<i>P2rx3</i>	-14.2	0.038
12	<i>P2ry2</i>	2.8	0.047
13	<i>P4ha3</i>	-3.4	0.004
14	<i>Pafah1b2</i>	-3.0	0.000
15	<i>Pafah2</i>	-104.0	0.004
16	<i>Pak1</i>	-3.7	0.001
17	<i>Pak3</i>	-4.6	0.039
18	<i>Palmd</i>	3.5	0.006
19	<i>Palmd</i>	3.5	0.006
20	<i>Pam16</i>	1.9	0.024
21	<i>Pam16</i>	1.9	0.024
22	<i>Pard3b</i>	2.4	0.024
23	<i>Pard6g</i>	-2.8	0.000
24	<i>Parl</i>	-1.6	0.015
25	<i>Parvg</i>	-41.7	0.009
26	<i>Pax8</i>	724.6	0.001
27	<i>Paxip1</i>	-2.0	0.039
28	<i>Pc</i>	-2.9	0.018
29	<i>Pc</i>	-2.9	0.018
30	<i>Pccb</i>	-1.8	0.006
31	<i>Pcdh18</i>	-2.2	0.033
32	<i>Pcdh9</i>	-11.9	0.001
33	<i>Pcdhga8</i>	55.3	0.029
34	<i>Pck2</i>	1.9	0.005
35	<i>Pcmtd1</i>	1.6	0.025
36	<i>Pcmtd2</i>	1.6	0.044
37	<i>Pcsk1</i>	1275.4	0.000
38	<i>Pcsk1</i>	1275.4	0.000
39	<i>Pde10a</i>	411.1	0.001
40	<i>Pde1b</i>	-291.6	0.018
41	<i>Pde4dip</i>	-2.1	0.006
42	<i>Pdia4</i>	-1.9	0.001
43	<i>Pdia6</i>	-2.2	0.000
44	<i>Pdk1</i>	-1.8	0.015
45	<i>Pdk1</i>	-1.8	0.015
46	<i>Pdlim2</i>	2.2	0.012

1	<i>Pdlim5</i>	-3.2	0.002
2	<i>Pdpr</i>	-235.7	0.002
3	<i>Pdxp</i>	-3.2	0.000
4	<i>Pdzd2</i>	4.2	0.014
5	<i>Pdzd7</i>	175.7	0.025
6	<i>Pecam1</i>	1.9	0.014
7	<i>Peg3</i>	-2.0	0.029
8	<i>Peg3</i>	-2.0	0.029
9	<i>Peli1</i>	-2.4	0.027
10	<i>Penk</i>	-2.4	0.020
11	<i>Per3</i>	-3.8	0.034
12	<i>Pet100</i>	1.6	0.037
13	<i>Pex11b</i>	-2.5	0.028
14	<i>Pex13</i>	-1.7	0.022
15	<i>Pex16</i>	2.3	0.001
16	<i>Pex26</i>	4.3	0.005
17	<i>Pex6</i>	2.0	0.042
18	<i>Pex7</i>	-8.9	0.001
19	<i>Pfdn6</i>	2.0	0.049
20	<i>Pgam2</i>	-21.0	0.036
21	<i>Pgbd5</i>	-410.6	0.008
22	<i>Pgg1b</i>	-3.7	0.014
23	<i>Pgp</i>	1.5	0.023
24	<i>Phb2</i>	-1.5	0.005
25	<i>Phkg1</i>	134.3	0.016
26	<i>Phkg2</i>	1.9	0.004
27	<i>Pias2</i>	-1.8	0.040
28	<i>Picalm</i>	-2.1	0.030
29	<i>Pid1</i>	-3.4	0.013
30	<i>Pigl</i>	6.8	0.002
31	<i>Pigm</i>	-6.7	0.016
32	<i>Pign</i>	-10.2	0.023
33	<i>Pigp</i>	2.8	0.000
34	<i>Pih1d2</i>	3.2	0.019
35	<i>Pik3c2a</i>	2.9	0.008
36	<i>Pik3c2g</i>	33.6	0.042
37	<i>Pik3cb</i>	27.4	0.011
38	<i>Pik3r1</i>	4.1	0.006
39	<i>Pim3</i>	2.5	0.000
40	<i>Pirt</i>	-175.4	0.015
41	<i>Pkd1</i>	2.0	0.015
42	<i>Pkdcc</i>	-2.0	0.006
43	<i>Pkig</i>	1.7	0.014
44	<i>Pknox2</i>	-19.6	0.023
45	<i>Pla2g12a</i>	2.6	0.027
46	<i>Pla2g5</i>	7.9	0.000

1	<i>Pla2g7</i>	4.0	0.046
2	<i>Plag1</i>	198.1	0.009
3	<i>Plcb2</i>	115.8	0.001
4	<i>Plcg1</i>	1.8	0.037
5	<i>Plec</i>	1.8	0.017
6	<i>Plekha3</i>	-1.5	0.036
7	<i>Plekha4</i>	6.0	0.034
8	<i>Plekha8</i>	2.4	0.045
9	<i>Plekhf1</i>	1.9	0.006
10	<i>Plekhn1</i>	867.1	0.001
11	<i>Plet1</i>	549.9	0.017
12	<i>Plg</i>	411.9	0.006
13	<i>Plin1</i>	80.0	0.021
14	<i>Plod3</i>	1.6	0.042
15	<i>PnISR</i>	2.3	0.003
16	<i>Pnpla7</i>	4.0	0.000
17	<i>Pof1b</i>	216.9	0.003
18	<i>Pold4</i>	1.6	0.026
19	<i>Poli</i>	21.1	0.020
20	<i>Polr1a,Rpa1</i>	#N/A	#N/A
21	<i>Polr2k</i>	2.5	0.004
22	<i>Polr2m</i>	-1.9	0.015
23	<i>Polr3e</i>	-2.6	0.002
24	<i>Pon2</i>	-2.0	0.005
25	<i>Pop5</i>	2.3	0.001
26	<i>Popdc3</i>	-332.3	0.012
27	<i>Porcn</i>	1.9	0.024
28	<i>Pot1</i>	-2.8	0.013
29	<i>Pou2af1</i>	-21.5	0.030
30	<i>Pou3f3</i>	39.6	0.035
31	<i>Ppa2</i>	-2.0	0.004
32	<i>Ppef2</i>	54.9	0.024
33	<i>Ppfia3</i>	-63.7	0.003
34	<i>Ppfibp2</i>	2.3	0.002
35	<i>Ppm1a</i>	-1.7	0.013
36	<i>Ppm1g</i>	-1.6	0.007
37	<i>Ppp1r10</i>	1.5	0.040
38	<i>Ppp1r14b</i>	1.6	0.032
39	<i>Ppp1r7</i>	-1.7	0.034
40	<i>Ppp1r8</i>	2.2	0.013
41	<i>Ppp1r9a</i>	52.8	0.044
42	<i>Ppp2ca</i>	-1.6	0.039
43	<i>Ppp2r1b</i>	-2.6	0.024
44	<i>Ppp2r5c</i>	-1.7	0.011
45	<i>Ppp3cc</i>	-2.4	0.003
46	<i>Ppp3r1</i>	-2.3	0.002

1	<i>Prdm2</i>	2.4	0.048
2	<i>Prdx3</i>	-1.6	0.015
3	<i>Prickle2</i>	-2.3	0.032
4	<i>Prkar1a</i>	-1.8	0.002
5	<i>Prkcd</i>	-2.4	0.001
6	<i>Prkcq</i>	-26.1	0.034
7	<i>Prkcsh</i>	1.6	0.003
8	<i>Prkx</i>	-3.5	0.007
9	<i>Prmt3</i>	-3.0	0.003
10	<i>Proc</i>	124.7	0.029
11	<i>Prokr2</i>	-167.6	0.000
12	<i>Prox2</i>	94.0	0.031
13	<i>Prpf18</i>	2.0	0.017
14	<i>Prpf38b</i>	1.6	0.033
15	<i>Prpf40a</i>	-1.5	0.005
16	<i>Prpf40b</i>	2.0	0.042
17	<i>Prps1</i>	-2.2	0.006
18	<i>Prr13</i>	1.8	0.005
19	<i>Prss12</i>	-5.3	0.000
20	<i>Prss30</i>	-129.5	0.037
21	<i>Prss8</i>	301.4	0.003
22	<i>Psat1</i>	-4.1	0.017
23	<i>Psmb10</i>	1.7	0.028
24	<i>Psmd3</i>	-1.6	0.016
25	<i>Pstpip1</i>	4.7	0.010
26	<i>Pstpip2</i>	-18.3	0.025
27	<i>Ptbp2</i>	-4.3	0.024
28	<i>Ptch2</i>	29.1	0.050
29	<i>Ptdss1</i>	-1.9	0.001
30	<i>Ptdss2</i>	-2.0	0.003
31	<i>Ptger2</i>	113.7	0.012
32	<i>Ptges</i>	-2.5	0.006
33	<i>Ptges3l1</i>	-12.4	0.008
34	<i>Ptgis</i>	4.1	0.000
35	<i>Ptgs1</i>	-3.8	0.008
36	<i>Ptgs2</i>	-225.2	0.012
37	<i>Ptk2</i>	-1.6	0.009
38	<i>Ptk7</i>	-1.5	0.046
39	<i>Ptp4a1</i>	-2.9	0.023
40	<i>Ptpn12</i>	2.1	0.018
41	<i>Ptpn2</i>	-1.8	0.027
42	<i>Ptpre</i>	3.2	0.004
43	<i>Ptprn</i>	183.4	0.013
44	<i>Ptprz1</i>	2.3	0.017
45	<i>Purb</i>	1.5	0.046
46	<i>Pvalb</i>	33.6	0.042

1	<i>Pwp2</i>	-2.8	0.029
2	<i>Pycr2</i>	1.6	0.004
3	<i>Pycrl</i>	-1.6	0.034
4	<i>Qdpr</i>	-1.7	0.039
5	<i>Rab18</i>	-1.6	0.024
6	<i>Rab1b</i>	-2.3	0.027
7	<i>Rab31</i>	1.6	0.033
8	<i>Rab39a</i>	63.9	0.021
9	<i>Rab3b</i>	123.6	0.023
10	<i>Rab5a</i>	-3.0	0.022
11	<i>Rab6b</i>	-5.4	0.045
12	<i>Rab8a</i>	-1.6	0.000
13	<i>Rabgap1l</i>	3.5	0.037
14	<i>Rabggta</i>	-2.0	0.029
15	<i>Rabggtb</i>	1.8	0.048
16	<i>Racgap1</i>	-6.0	0.004
17	<i>Rag1</i>	-28.2	0.044
18	<i>Rag2</i>	-559.7	0.006
19	<i>Ralbp1</i>	1.8	0.026
20	<i>Raly</i>	-1.6	0.002
21	<i>Ramp1</i>	2.3	0.000
22	<i>Rap1b</i>	-2.0	0.031
23	<i>Rapgef6</i>	-3.3	0.025
24	<i>Rarb</i>	-6.7	0.006
25	<i>Rasal1</i>	681.4	0.002
26	<i>Raver1</i>	-1.8	0.008
27	<i>Rbbp7</i>	-1.9	0.002
28	<i>Rbbp9</i>	-2.4	0.023
29	<i>Rbp2</i>	106.2	0.035
30	<i>Rbp2</i>	106.2	0.035
31	<i>Rbsn</i>	-2.1	0.036
32	<i>Rcbtb1</i>	-2.9	0.020
33	<i>Rcl1</i>	-2.0	0.038
34	<i>Rcl1,Clns1a</i>	#N/A	#N/A
35	<i>Rcor1</i>	1.7	0.011
36	<i>Rdh12</i>	227.6	0.003
37	<i>Rdm1</i>	1.9	0.042
38	<i>Reep2</i>	46.7	0.012
39	<i>Reep4</i>	2.0	0.025
40	<i>Reep5</i>	1.5	0.006
41	<i>Reln</i>	-14.2	0.048
42	<i>Rem2</i>	33.0	0.040
43	<i>Rev1</i>	-2.0	0.012
44	<i>R fwd2</i>	-1.8	0.001
45	<i>Rfx6</i>	39.6	0.039
46	<i>RGD1309730</i>	1.8	0.023

1	<i>RGD1311892</i>	64.8	0.030
2	<i>RGD1560436</i>	-96.7	0.031
3	<i>RGD1561102</i>	-168.7	0.025
4	<i>RGD1564379</i>	-1.6	0.009
5	<i>Rgs10</i>	2.0	0.009
6	<i>Rgs18</i>	-43.7	0.000
7	<i>Rgs2</i>	-2.5	0.010
8	<i>Rgs3</i>	2.0	0.003
9	<i>Rgs7</i>	-146.2	0.041
10	<i>Rhd</i>	-19.7	0.005
11	<i>Rhoh</i>	-7.6	0.025
12	<i>Rhot2</i>	2.7	0.006
13	<i>Rims2</i>	-197.4	0.003
14	<i>Ring1</i>	1.6	0.022
15	<i>Riok2</i>	-1.9	0.039
16	<i>Rita1</i>	2.6	0.003
17	<i>Rnaseh1</i>	2.0	0.040
18	<i>Rnaseh2a</i>	2.2	0.002
19	<i>Rnaseh2b</i>	-2.0	0.010
20	<i>Rnf111</i>	1.8	0.040
21	<i>Rnf114</i>	-1.6	0.002
22	<i>Rnf11/1</i>	-2.7	0.006
23	<i>Rnf123</i>	-2.1	0.009
24	<i>Rnf13</i>	-3.1	0.049
25	<i>Rnf2</i>	-2.0	0.002
26	<i>Rnf215</i>	1.7	0.041
27	<i>Rnf39</i>	148.1	0.010
28	<i>Rnf4</i>	-5.5	0.000
29	<i>Rnmt</i>	-1.9	0.009
30	<i>Robo1</i>	-4.2	0.023
31	<i>Rogdi</i>	-1.7	0.047
32	<i>Rpa1</i>	-7.4	0.002
33	<i>Rpa1</i>	-7.4	0.002
34	<i>Rpain</i>	2.1	0.014
35	<i>Rpf2</i>	-1.8	0.049
36	<i>Rpgrip1l</i>	3.4	0.023
37	<i>Rpl37a</i>	-16.5	0.043
38	<i>Rpn1</i>	-1.5	0.001
39	<i>Rpp21</i>	1.8	0.005
40	<i>Rpp25</i>	-64.6	0.001
41	<i>Rps17</i>	2.7	0.010
42	<i>Rps6ka3</i>	-3.8	0.000
43	<i>Rps6kb1</i>	-1.7	0.046
44	<i>Rragc</i>	-1.7	0.009
45	<i>Rras</i>	1.6	0.025
46	<i>Rreb1</i>	2.3	0.045

1	<i>Rrn3</i>	-3.0	0.046
2	<i>Rrp8</i>	-3.7	0.010
3	<i>Rsad2</i>	-13.6	0.007
4	<i>Rsl24d1</i>	-2.0	0.009
5	<i>Rtkn2</i>	-33.4	0.046
6	<i>Rtn4rl1</i>	3.1	0.011
7	<i>Runx1</i>	-3.3	0.012
8	<i>Ruvbl2</i>	-1.7	0.023
9	<i>S100a10</i>	2.4	0.005
10	<i>S100a16</i>	1.9	0.006
11	<i>S100a3</i>	2.3	0.044
12	<i>S100a4</i>	4.3	0.007
13	<i>S100a6</i>	4.5	0.002
14	<i>Sag</i>	36.1	0.026
15	<i>Sag</i>	36.1	0.026
16	<i>Sag</i>	36.1	0.026
17	<i>Sat1</i>	1.7	0.008
18	<i>Sat1</i>	1.7	0.008
19	<i>Sat1</i>	1.7	0.008
20	<i>Saxo2</i>	331.9	0.017
21	<i>Sbds</i>	1.7	0.016
22	<i>Sbf1</i>	1.8	0.034
23	<i>Sbsn</i>	13.7	0.002
24	<i>Scap</i>	1.8	0.028
25	<i>Scara5</i>	11.9	0.001
26	<i>Scd2</i>	-2.1	0.008
27	<i>Scfd1</i>	-1.8	0.002
28	<i>Scg5</i>	331.0	0.004
29	<i>Scgb1a1</i>	383.4	0.005
30	<i>Scn2b</i>	-11.1	0.039
31	<i>Scube3</i>	-33.8	0.023
32	<i>Sdcbp</i>	-1.5	0.026
33	<i>Sdcbp2</i>	-144.5	0.041
34	<i>Sdha</i>	-2.0	0.002
35	<i>Sdr16c5</i>	259.0	0.013
36	<i>Sec13</i>	-1.7	0.002
37	<i>Sec14l1</i>	3.1	0.000
38	<i>Sec22b</i>	-2.3	0.000
39	<i>Sec23ip</i>	-2.1	0.003
40	<i>Sec24a</i>	-3.9	0.017
41	<i>Sec61a2</i>	-2.3	0.002
42	<i>Selk</i>	1.8	0.004
43	<i>Selt</i>	-1.6	0.002
44	<i>Sema3e</i>	37.2	0.032
45	<i>Sema4b</i>	-3.0	0.004
46	<i>Serp1</i>	-2.0	0.000

1	<i>Serpib10</i>	18.3	0.037
2	<i>Serpib2</i>	549.6	0.001
3	<i>Serpib8</i>	331.2	0.000
4	<i>Serpib9</i>	-2.3	0.022
5	<i>Serpine1</i>	7.0	0.001
6	<i>Serpine2</i>	-2.1	0.022
7	<i>Sesn1</i>	-2.3	0.011
8	<i>Set</i>	-1.8	0.009
9	<i>Sf3a2</i>	-1.9	0.017
10	<i>Sf3b4</i>	-1.6	0.037
11	<i>Sfi1</i>	2.2	0.026
12	<i>Sfmbt2</i>	-147.8	0.038
13	<i>Sftpc</i>	117.9	0.019
14	<i>Sfxn1</i>	-4.0	0.003
15	<i>Sfxn3</i>	1.5	0.012
16	<i>Sgcd</i>	-2.0	0.036
17	<i>Sgpl1</i>	-6.0	0.010
18	<i>Sh2d2a</i>	-375.9	0.009
19	<i>Sh3glb2</i>	2.2	0.001
20	<i>Shc4</i>	92.0	0.022
21	<i>Shmt1</i>	-7.7	0.007
22	<i>Shpk</i>	561.9	0.000
23	<i>Shtn1</i>	14.8	0.005
24	<i>Siglec10</i>	-20.9	0.010
25	<i>Sirt3</i>	4.8	0.000
26	<i>Sirt4</i>	2.8	0.038
27	<i>Sit1</i>	-11.4	0.033
28	<i>Sit1,Slc6a20</i>	#N/A	#N/A
29	<i>Skp2</i>	-2.3	0.033
30	<i>Slamf7</i>	-169.8	0.005
31	<i>Slbp</i>	-1.6	0.042
32	<i>Slc12a4</i>	1.7	0.020
33	<i>Slc13a5</i>	3.6	0.029
34	<i>Slc15a2</i>	78.1	0.010
35	<i>Slc15a3</i>	2.6	0.020
36	<i>Slc16a1</i>	-6.2	0.001
37	<i>Slc16a13</i>	3.9	0.036
38	<i>Slc16a14</i>	45.4	0.036
39	<i>Slc16a2</i>	-5.1	0.026
40	<i>Slc1a1</i>	167.2	0.007
41	<i>Slc1a2</i>	244.6	0.008
42	<i>Slc1a3</i>	-5.5	0.000
43	<i>Slc1a6</i>	-35.1	0.014
44	<i>Slc24a4</i>	-21.9	0.032
45	<i>Slc25a23</i>	44.0	0.019
46	<i>Slc25a25</i>	-2.9	0.008

1	<i>Slc25a28</i>	1.9	0.002
2	<i>Slc25a46</i>	-1.8	0.013
3	<i>Slc26a6</i>	4.1	0.013
4	<i>Slc28a1</i>	259.0	0.018
5	<i>Slc28a3</i>	124.1	0.009
6	<i>Slc30a10</i>	-41.1	0.038
7	<i>Slc30a3</i>	-279.3	0.012
8	<i>Slc30a6</i>	-2.3	0.014
9	<i>Slc30a7</i>	-2.0	0.021
10	<i>Slc35e4</i>	2.3	0.008
11	<i>Slc39a1</i>	3.1	0.021
12	<i>Slc39a14</i>	2.0	0.048
13	<i>Slc39a3</i>	2.7	0.000
14	<i>Slc39a8</i>	-2.4	0.008
15	<i>Slc43a2</i>	3.4	0.006
16	<i>Slc4a9</i>	320.0	0.005
17	<i>Slc52a3</i>	45.5	0.029
18	<i>Slc5a5</i>	-307.9	0.015
19	<i>Slc5a9</i>	248.0	0.027
20	<i>Slc6a8</i>	2.6	0.007
21	<i>Slc7a10</i>	-229.0	0.018
22	<i>Slc7a3</i>	60.1	0.042
23	<i>Slc8b1</i>	3.2	0.002
24	<i>Slc9a3</i>	83.1	0.011
25	<i>Slc9a8</i>	-5.8	0.011
26	<i>Slc9a9</i>	-2.7	0.025
27	<i>Slco4a1</i>	16.9	0.037
28	<i>Slit3</i>	2.5	0.002
29	<i>Slmo2</i>	-1.8	0.001
30	<i>Slx1b</i>	2.3	0.001
31	<i>Smad2</i>	-2.1	0.009
32	<i>Smad6</i>	1.9	0.044
33	<i>Smad7</i>	2.6	0.012
34	<i>Smagp</i>	2.1	0.033
35	<i>Smarcc1</i>	-2.3	0.004
36	<i>Smarcd1</i>	-1.6	0.034
37	<i>Smpd2</i>	1.9	0.028
38	<i>Snai2</i>	-2.4	0.006
39	<i>Snai3</i>	192.9	0.009
40	<i>Snca</i>	-7.8	0.031
41	<i>Snn</i>	-2.3	0.047
42	<i>Snrpd2</i>	1.6	0.042
43	<i>Snta1</i>	2.0	0.005
44	<i>Sntb1</i>	83.1	0.018
45	<i>Sntg2</i>	-216.3	0.019
46	<i>Snx6</i>	-1.7	0.000

1	<i>Snx9</i>	-2.1	0.021
2	<i>Soat1</i>	-11.8	0.000
3	<i>Sox12</i>	-2.0	0.050
4	<i>Sp9</i>	-6.4	0.018
5	<i>Spib</i>	-22.8	0.001
6	<i>Spn</i>	9.9	0.002
7	<i>Spn</i>	9.9	0.002
8	<i>Spp1</i>	7.7	0.002
9	<i>Spp1</i>	7.7	0.002
10	<i>Spred3</i>	86.8	0.011
11	<i>Sprr1a</i>	2654.6	0.001
12	<i>Spry1</i>	2.1	0.029
13	<i>Spsb1</i>	-4.0	0.018
14	<i>Spsb4</i>	-59.9	0.007
15	<i>Spta1</i>	-7.7	0.043
16	<i>Sptbn1</i>	1.8	0.027
17	<i>Srd5a1</i>	-14.7	0.006
18	<i>Srebf2</i>	1.8	0.000
19	<i>Srf</i>	2.6	0.005
20	<i>Srp14</i>	1.6	0.002
21	<i>Srpk3</i>	-104.9	0.001
22	<i>Srprb</i>	-1.6	0.044
23	<i>Srrm2</i>	1.9	0.023
24	<i>Srsf1</i>	-1.5	0.023
25	<i>Srsf11</i>	1.8	0.005
26	<i>Srsf4</i>	-1.7	0.045
27	<i>Srsf5</i>	-2.3	0.000
28	<i>Sspo</i>	171.3	0.015
29	<i>Sstr2</i>	71.9	0.028
30	<i>St14</i>	2.7	0.033
31	<i>St3gal2</i>	1.9	0.004
32	<i>St6galnac2</i>	-2.5	0.001
33	<i>St8sia2</i>	-438.7	0.005
34	<i>Stac2</i>	-289.1	0.012
35	<i>Stamp</i>	-2.3	0.010
36	<i>Stard7</i>	-3.4	0.013
37	<i>Steap3</i>	1.9	0.032
38	<i>Stip1</i>	-1.7	0.049
39	<i>Stip1</i>	-1.7	0.049
40	<i>Stk26</i>	-17.3	0.009
41	<i>Stk35</i>	-3.6	0.014
42	<i>Stmn2</i>	69.6	0.043
43	<i>Strada</i>	-2.0	0.034
44	<i>Stt3b</i>	-3.0	0.003
45	<i>Stx6</i>	-1.7	0.047
46	<i>Stx7</i>	-2.5	0.011

1	<i>Sulf1</i>	3.6	0.001
2	<i>Sult1a1</i>	2.7	0.047
3	<i>Sult2b1</i>	119.1	0.023
4	<i>Sumf2</i>	-1.8	0.038
5	<i>Sumo1</i>	-1.6	0.000
6	<i>Sumo2</i>	-1.7	0.014
7	<i>Suv420h1</i>	2.0	0.014
8	<i>Sv2b</i>	69.2	0.005
9	<i>Svil</i>	2.4	0.005
10	<i>Swt1</i>	2.1	0.019
11	<i>Sympk</i>	-1.9	0.033
12	<i>Syn3</i>	-170.5	0.023
13	<i>Syndig1</i>	12.4	0.044
14	<i>Syne3</i>	58.2	0.001
15	<i>Synm</i>	4.3	0.011
16	<i>Syt1</i>	101.3	0.020
17	<i>Syt17</i>	36.4	0.040
18	<i>Syt4</i>	-47.4	0.042
19	<i>Syt6</i>	-100.7	0.028
20	<i>Syt8</i>	189.1	0.019
21	<i>Syvn1</i>	-1.5	0.033
22	<i>Tacc1</i>	1.6	0.014
23	<i>Tacr1</i>	250.9	0.011
24	<i>Tacstd2</i>	475.5	0.007
25	<i>Taf1a</i>	-4.5	0.016
26	<i>Taf9b</i>	-1.9	0.038
27	<i>Tars</i>	-2.2	0.020
28	<i>Tas1r1</i>	-96.2	0.027
29	<i>Tatdn2</i>	1.7	0.029
30	<i>Tbc1d10a</i>	1.7	0.024
31	<i>Tbc1d10b</i>	-1.7	0.026
32	<i>Tbc1d20</i>	-2.5	0.004
33	<i>Tbp</i>	-2.3	0.006
34	<i>Tbx15</i>	-75.4	0.045
35	<i>Tbx2r</i>	-3.4	0.004
36	<i>Tcf12</i>	-2.3	0.007
37	<i>Tcirg1</i>	2.1	0.015
38	<i>Tcp1</i>	-2.3	0.007
39	<i>Tdh</i>	149.3	0.015
40	<i>Tdp2</i>	2.1	0.007
41	<i>Tefm</i>	-6.9	0.000
42	<i>Tenm2</i>	-36.6	0.049
43	<i>Tep1</i>	2.8	0.004
44	<i>Tesk1</i>	1.8	0.008
45	<i>Tesk2</i>	-6.4	0.030
46	<i>Tf</i>	-5.4	0.010

1	<i>Tf</i>	-5.4	0.010
2	<i>Tfap2e</i>	93.3	0.038
3	<i>Tfb1m</i>	1.9	0.045
4	<i>Tgif2</i>	-3.6	0.048
5	<i>Thbs4</i>	4.4	0.001
6	<i>Thoc3</i>	-1.6	0.022
7	<i>Thoc5</i>	-2.1	0.008
8	<i>Thrap3</i>	-1.8	0.025
9	<i>Thsd7b</i>	-50.1	0.016
10	<i>Tiam1</i>	45.1	0.000
11	<i>Tifa</i>	-7.3	0.000
12	<i>Timd2</i>	127.6	0.002
13	<i>Timm13</i>	1.8	0.011
14	<i>Timm8b</i>	1.6	0.043
15	<i>Tiprl</i>	-2.1	0.003
16	<i>Tjp1</i>	1.9	0.045
17	<i>Tkfc</i>	-2.6	0.028
18	<i>Tle1</i>	-2.8	0.005
19	<i>Tle4</i>	-2.2	0.016
20	<i>Tlr2</i>	-4.3	0.033
21	<i>Tlr4</i>	248.7	0.000
22	<i>Tmed2</i>	-1.8	0.002
23	<i>Tmeff1</i>	-3.0	0.004
24	<i>Tmem109</i>	1.6	0.010
25	<i>Tmem135</i>	-2.7	0.042
26	<i>Tmem170b</i>	365.8	0.003
27	<i>Tmem178a</i>	-15.2	0.010
28	<i>Tmem208</i>	1.7	0.017
29	<i>Tmem259</i>	2.0	0.009
30	<i>Tmem33</i>	2.0	0.021
31	<i>Tmem43</i>	-1.8	0.004
32	<i>Tmem71</i>	-23.7	0.034
33	<i>Tmem80</i>	2.1	0.039
34	<i>Tmem86b</i>	-12.1	0.021
35	<i>Tmem9</i>	-1.9	0.001
36	<i>Tmod4</i>	22.6	0.032
37	<i>Tmprss11d</i>	394.4	0.009
38	<i>Tmprss3</i>	-99.9	0.014
39	<i>Tmprss6</i>	-94.3	0.029
40	<i>Tmprss9</i>	12.5	0.040
41	<i>Tmsb4x</i>	2.0	0.002
42	<i>Tmtc2</i>	-4.1	0.017
43	<i>Tmx1</i>	-1.9	0.044
44	<i>Tnfaip1</i>	-2.3	0.001
45	<i>Tnfrsf13b</i>	-52.3	0.024
46	<i>Tnfrsf14</i>	18.2	0.018

1	<i>Tnfrsf18</i>	-240.7	0.012
2	<i>Tnfrsf19</i>	-3.0	0.001
3	<i>Tnfsf13b</i>	-98.6	0.029
4	<i>Tnmd</i>	-5.4	0.003
5	<i>Tnncl</i>	-38.0	0.003
6	<i>Tnncl2</i>	964.7	0.002
7	<i>Tnni1</i>	45.5	0.038
8	<i>Tnrc18</i>	2.2	0.015
9	<i>Tnrc6b</i>	2.2	0.006
10	<i>Tns3</i>	1.8	0.030
11	<i>Tob1</i>	2.5	0.014
12	<i>Tom1l1</i>	-3.4	0.008
13	<i>Tox</i>	12.5	0.045
14	<i>Tox4</i>	-2.0	0.002
15	<i>Tp53i13</i>	1.6	0.009
16	<i>Tp53inp2</i>	1.7	0.031
17	<i>Tpm1</i>	-2.2	0.000
18	<i>Tpm4</i>	-2.2	0.001
19	<i>Tpp1</i>	1.8	0.037
20	<i>Tpp1</i>	1.8	0.037
21	<i>Tppp3</i>	3.5	0.018
22	<i>Tpra1</i>	1.6	0.012
23	<i>Tra2b</i>	-1.5	0.010
24	<i>Trappc1</i>	-1.5	0.003
25	<i>Trappc4</i>	1.9	0.002
26	<i>Trex1</i>	2.3	0.002
27	<i>Trib2</i>	2.4	0.002
28	<i>Trim13</i>	-17.1	0.020
29	<i>Trim21</i>	-46.9	0.012
30	<i>Trim37</i>	-2.7	0.038
31	<i>Trim47</i>	2.3	0.002
32	<i>Trim54</i>	187.0	0.013
33	<i>Trim59</i>	-2.1	0.040
34	<i>Trim69</i>	217.0	0.014
35	<i>Trim8</i>	1.5	0.022
36	<i>Trip6</i>	2.0	0.003
37	<i>Trmt10b</i>	2.0	0.030
38	<i>Trmt10c</i>	-1.6	0.036
39	<i>Trpm1</i>	105.4	0.018
40	<i>Trpm8</i>	-100.5	0.019
41	<i>Trpv6</i>	116.7	0.013
42	<i>Trub1</i>	-6.7	0.010
43	<i>Tsacc</i>	99.9	0.018
44	<i>Tspan17</i>	1.9	0.048
45	<i>Tspan6</i>	-1.8	0.002
46	<i>Tspo</i>	2.4	0.001

1	<i>Tspy1</i>	-1.5	0.014
2	<i>Ttbk2</i>	4.0	0.027
3	<i>Ttc12</i>	75.4	0.013
4	<i>Ttc17</i>	2.6	0.033
5	<i>Ttf2</i>	2.0	0.031
6	<i>Ttll10</i>	112.0	0.025
7	<i>Ttll3</i>	11.4	0.043
8	<i>Ttyh3</i>	-1.7	0.012
9	<i>Tuba8</i>	199.0	0.000
10	<i>Tubb2a</i>	1.9	0.011
11	<i>Tubb2a</i>	1.9	0.011
12	<i>Tubb4a</i>	222.6	0.014
13	<i>Tubgcp3</i>	2.8	0.006
14	<i>Tusc2</i>	1.6	0.003
15	<i>Txlna</i>	-1.9	0.020
16	<i>Txndc5</i>	-1.5	0.021
17	<i>Tyms</i>	-2.2	0.025
18	<i>Tyrobp</i>	2.3	0.035
19	<i>Uba1</i>	-1.5	0.032
20	<i>Uba2</i>	-3.0	0.020
21	<i>Ubac2</i>	-2.0	0.000
22	<i>Ubash3a</i>	-67.6	0.025
23	<i>Ubc</i>	1.7	0.002
24	<i>Ubd</i>	-72.8	0.047
25	<i>Ube2v2</i>	-1.8	0.003
26	<i>Ubxn2b</i>	-7.3	0.011
27	<i>Ubxn6</i>	1.6	0.004
28	<i>Uchl1</i>	-3.3	0.001
29	<i>Ucp3</i>	494.6	0.008
30	<i>Ugcg</i>	-2.5	0.011
31	<i>Ugdh</i>	-1.8	0.015
32	<i>Uhrf1</i>	-7.7	0.015
33	<i>Umps</i>	-1.8	0.003
34	<i>Unc45a</i>	2.3	0.000
35	<i>Unc5a</i>	770.6	0.007
36	<i>Unc5c</i>	3.7	0.010
37	<i>Unc5d</i>	-35.1	0.046
38	<i>Uqcc1</i>	-1.8	0.039
39	<i>Uqcr11</i>	1.8	0.005
40	<i>Uqcrq</i>	1.6	0.034
41	<i>Urb1</i>	3.3	0.033
42	<i>Use1</i>	2.0	0.003
43	<i>Use1,Ube2z</i>	#N/A	#N/A
44	<i>Usmg5</i>	2.0	0.028
45	<i>Usp11</i>	-3.7	0.000
46	<i>Usp14</i>	-1.5	0.026

1	<i>Usp19</i>	1.8	0.041
2	<i>Usp24</i>	2.6	0.019
3	<i>Usp33</i>	2.5	0.024
4	<i>Usp36</i>	2.2	0.030
5	<i>Vac14</i>	-2.1	0.009
6	<i>Vamp5</i>	2.2	0.015
7	<i>Vamp8</i>	2.0	0.000
8	<i>Vapb</i>	-2.0	0.006
9	<i>Vil1</i>	-119.4	0.031
10	<i>Vim</i>	1.9	0.005
11	<i>Vipas39</i>	2.2	0.006
12	<i>Vmac</i>	-3.0	0.032
13	<i>Vps13a</i>	4.7	0.008
14	<i>Vps13d</i>	3.3	0.002
15	<i>Vps26a</i>	-2.1	0.021
16	<i>Vps35</i>	-1.7	0.014
17	<i>Vps37b</i>	-2.1	0.013
18	<i>Vps41</i>	-2.4	0.000
19	<i>Vps52</i>	-1.8	0.048
20	<i>Vps53</i>	1.9	0.033
21	<i>Vrk2</i>	-3.5	0.012
22	<i>Vti1a</i>	-4.4	0.001
23	<i>Wars2</i>	-5.0	0.047
24	<i>Wasf2</i>	1.6	0.028
25	<i>Wasl</i>	1.6	0.041
26	<i>Wdfy3</i>	2.8	0.009
27	<i>Wdr5</i>	-1.7	0.035
28	<i>Wdr6</i>	-1.8	0.046
29	<i>Wdr75</i>	-2.9	0.000
30	<i>Wisp2</i>	7.6	0.020
31	<i>Wls</i>	-1.6	0.034
32	<i>Wnt11</i>	-3.2	0.009
33	<i>Wnt5b</i>	2.6	0.004
34	<i>Wrap73</i>	1.7	0.042
35	<i>Xk</i>	-35.6	0.018
36	<i>Xkr4</i>	33.9	0.034
37	<i>Xkr6</i>	32.9	0.034
38	<i>Xpo1</i>	-2.2	0.025
39	<i>Xpo6</i>	-2.2	0.008
40	<i>Xpot</i>	-2.2	0.012
41	<i>Xrcc1</i>	1.8	0.002
42	<i>Xrcc5</i>	-2.6	0.001
43	<i>Yaf2</i>	-1.6	0.015
44	<i>Ykt6</i>	-2.6	0.006
45	<i>Ylpm1</i>	1.8	0.045
46	<i>Ythdc1</i>	2.0	0.025

1	<i>Ywhab</i>	-1.5	0.002
2	<i>Ywhae</i>	-1.7	0.000
3	<i>Ywhag</i>	1.7	0.014
4	<i>Ywhaz</i>	-1.7	0.004
5	<i>Zbed3</i>	-1.7	0.036
6	<i>Zbp1</i>	-40.1	0.026
7	<i>Zbp1</i>	-40.1	0.026
8	<i>Zbtb16</i>	337.2	0.001
9	<i>Zbtb7c</i>	3.5	0.018
10	<i>Zc3h10</i>	2.6	0.002
11	<i>Zc3h14</i>	-1.9	0.010
12	<i>Zcchc12</i>	-3.4	0.008
13	<i>Zcrb1</i>	1.5	0.025
14	<i>Zdhhc20</i>	-2.4	0.001
15	<i>Zdhhc6</i>	-1.9	0.012
16	<i>Zfp2</i>	247.2	0.005
17	<i>Zfp263</i>	-2.3	0.019
18	<i>Zfp280b</i>	9.6	0.029
19	<i>Zfp394</i>	2.1	0.045
20	<i>Zfp410</i>	-1.7	0.030
21	<i>Zfp422</i>	-1.9	0.003
22	<i>Zfp467</i>	2.3	0.031
23	<i>Zfp483</i>	-181.1	0.023
24	<i>Zfp513</i>	1.8	0.041
25	<i>Zfp521</i>	-2.2	0.018
26	<i>Zfp641</i>	27.7	0.033
27	<i>Zfp68</i>	-2.0	0.012
28	<i>Zgpat</i>	2.4	0.027
29	<i>Zim1</i>	-290.1	0.014
30	<i>Zmpste24</i>	-5.5	0.000
31	<i>Znhit1</i>	1.9	0.012
32	<i>Znrd1</i>	1.7	0.037
33	<i>Zpbp</i>	-114.6	0.006
34	<i>Zswim5</i>	184.5	0.008
35			
36			
37			
38			
39			
40			
41			
42			
43			
44			
45			
46			
47			
48			
49			
50			
51			
52			
53			
54			
55			
56			
57			
58			
59			
60			

Appendix Table 2

The original proteomic analysis data of stretched PDL cells showed in Figure 4.

Accession	Gene	LFQ intensity Control	LFQ intensity Stretched
A0A024R442	DNPEP	0	20.9996891
A0A075B785	RELCH	0	19.76844597
A0A087WTA8	COL1A2	25.22523308	26.31858635
A0A087WVZ9	POLR2E	0	20.16643715
A0A087WX58	HDGFL2	0	19.65448952
A0A087WXC5	NDUFA10	22.09055138	0
A0A087WYV8	FBN2	19.73524284	20.74386215
A0A0A0MRE1	EXOC7	0	20.59914207
A0A0A0MSK4	GPSM1	21.75103188	20.19568443
A0A0A0MTN9	FDXR	0	20.98454094
A0A0A0MTR7	RNF213	23.30827522	24.40379715
	TMED7-		
A0A0A6YYA0	TICAM2	21.09119797	22.54521751
A0A0B4J2A0	None	0	19.78540421
A0A0C4DFM1	TM9SF4	21.73148537	20.58682823
A0A0C4DG40	SYNE1	23.24419022	24.31257439
A0A0G2JNZ5	GBA	0	22.26023293
A0A0U1RR22	PAC SIN2	0	22.15375519
A0A1B0GTU1	ZC3H11B	0	17.82059097
A0A1B0GWF2	STXBP1	20.82973862	22.27295685
A0A1W2PR68	ME2	0	19.77781677
A0A2R8Y430	GSS	0	22.14416885
A0A2R8YF43	CSNK2A1	22.16628456	21.01202202
A0A3B3IS01	DARS2	19.57568359	0
B1ALD9	POSTN	21.65460205	20.32410622
B1ANM7	FAF1	21.37023354	20.30463219
B4E1E4	EIF4E2	0	19.40582275
B8ZZC5	GLS	20.10686874	0
C9JBI3	PSPH	0	18.98061371
C9JJ54	WDFY1	19.68905258	0
E7EWK3	DHX36	0	20.04686737
E9PB90	HK2	22.67480278	21.65110207
E9PF19	TBL2	21.46188927	20.36474228
E9PGM1	EIF4G1	26.33698273	24.98767471
E9PHV5	ITPRID2	19.72468948	20.93531418
E9PKU7	GANAB	0	20.05959702
E9PLK3	NPEPPS	24.54639626	25.80466843
E9PNL4	STX5	0	20.20741081
E9PQP3	ARFGAP2	0	19.80453111
F2Z2X4	XPO4	0	19.36851883
F5H4B6	ALDH16A1	20.39947319	0

1	F5H5N1	NDUFS7	0	20.1316967
2	F8VSC5	SCYL2	0	20.32432556
3	F8W020	NAP1L1	23.19088554	24.30340576
4	F8W1F5	FMNL3	0	19.6111908
5	F8W808	NAA10	21.89081955	20.4582386
6	F8W9T3	SNX4	0	21.89969635
7	G3V126	ATP6V1H	0	18.98281479
8	G3V529	DDX24	0	18.44596863
9	G5E9S8	KLC1	23.14177132	24.31741333
10	H0YDP7	MRPL49	0	20.50581551
11	J3KTF8	ARHGDIA	24.56307983	25.60501099
12	J3QLR8	MRPS23	0	19.49917221
13	J3QR09	RPL19	22.55912781	23.77283669
14	M0R026	ILVBL	21.18252945	19.68642235
15	M0R208	CLPP	20.40789795	22.10980606
16	O00267	SUPT5H	0	20.00237083
17	O00754	MAN2B1	0	20.7157383
18	O14818	PSMA7	24.01154327	25.14390373
19	O15173	PGRMC2	22.74915123	23.92315865
20	O15270	SPTLC2	0	19.53425407
21	O15427	SLC16A3	23.23410606	22.17292023
22	O15460	P4HA2	24.34638023	26.01073265
23	O43390	HNRNPR	21.59418488	23.08321571
24	O60502	OGA	0	21.01352119
25	O60762	DPM1	19.60188293	20.8239994
26	O75534	CSDE1	21.91338539	22.95976639
27	O75643	SNRNP200	26.44395256	25.00906754
28	O75844	ZMPSTE24	21.97571754	20.68953133
29	O75962	TRIO	20.65394783	21.80644417
30	O75976	CPD	0	21.04092979
31	O94804	STK10	0	17.59433937
32	O95197	RTN3	22.27332687	20.819561
33	O95248	SBF1	0	21.51123238
34	O95810	CAVIN2	0	19.57767677
35	O95881	TXNDC12	0	20.94177628
36	O96005	CLPTM1	22.37983513	21.17718506
37	P02452	COL1A1	26.02312088	28.7821312
38	P02461	COL3A1	21.85866928	23.9216156
39	P02545	LMNA	28.88495064	29.89865112
40	P02792	FTL	23.62644958	22.54158401
41	P04080	CSTB	23.54957199	22.35901451
42	P04632	CAPNS1	24.03204155	25.27476311
43	P04792	HSPB1	26.62714577	27.82420158
44	P04818	TYMS	21.41142082	20.24898911
45	P05997	COL5A2	19.73646545	21.18924332
46	P07814	EPRS	24.96146393	26.25281143
47	P08243	ASNS	22.13842964	23.32909775

1	P08574	CYC1	0	20.90873909
2	P08648	ITGA5	25.22574806	24.18737221
3	P09960	LTA4H	21.50149727	22.81188202
4	P0DMV9	HSPA1B	29.0905323	27.32551575
5	P12081	HARS	24.30528641	25.34235001
6	P14923	JUP	20.95695114	0
7	P15104	GLUL	0	20.75287056
8	P16234	PDGFRA	0	20.9249897
9	P16930	FAH	21.85178566	20.74779892
10	P17066	HSPA6	28.77596092	27.75748062
11	P19174	PLCG1	0	19.5958519
12	P19474	TRIM21	0	19.35287476
13	P20908	COL5A1	21.16090965	22.27810097
14	P21964	COMT	22.38226509	23.46811867
15	P23381	WARS	23.40743256	24.44335365
16	P24928	POLR2A	20.53763199	19.08085442
17	P26022	PTX3	0	19.87612724
18	P26038	MSN	28.74890327	29.82072258
19	P26373	RPL13	25.4160614	26.60385323
20	P27348	YWHAQ	26.22118187	27.4228611
21	P28288	ABCD3	21.29283142	19.83644104
22	P30038	ALDH4A1	0	18.69149208
23	P30405	PPIF	23.03175545	22.02116776
24	P31153	MAT2A	23.43478966	22.30924797
25	P32119	PRDX2	25.56575584	24.35137749
26	P32455	GBP1	20.91342163	22.04620171
27	P35354	PTGS2	22.50054932	20.74246407
28	P35573	AGL	0	18.90124321
29	P42167	TMPO	20.45352364	21.76198578
30	P43487	RANBP1	22.69242859	23.94628143
31	P46821	MAP1B	27.4512043	26.03632545
32	P46937	YAP1	21.46173859	22.57327652
33	P46940	IQGAP1	27.27382088	28.48834229
34	P47914	RPL29	23.20067596	24.29459953
35	P49748	ACADVL	25.07842827	26.20894051
36	P50395	GDI2	26.025383	27.03128433
37	P50416	CPT1A	23.39610672	22.20943451
38	P51809	VAMP7	0	19.97687149
39	P51970	NDUFA8	21.54297638	19.81770515
40	P52630	STAT2	20.81151009	21.92524338
41	P55084	HADHB	25.01979446	23.79213333
42	P56545	CTBP2	21.70956612	22.81381989
43	P57764	GSDMD	0	19.04390907
44	P61586	RHOA	0	22.79070282
45	P61619	SEC61A1	24.79808044	23.63533401
46	P62826	RAN	25.3025341	26.37102509
47	P67809	YBX1	25.56435966	24.45349884

1	P78559	MAP1A	23.87107658	24.99183273
2	Q00688	FKBP3	21.51638603	23.73106956
3	Q04917	YWHAH	24.16622353	25.20988846
4	Q06124	PTPN11	21.06716919	22.37581062
5	Q06203	PPAT	0	20.50057411
6	Q08378	GOLGA3	21.67620277	22.77782059
7	Q12965	MYO1E	20.13746071	21.31959343
8	Q13131	PRKAA1	0	21.00422287
9	Q13242	SRSF9	19.10469627	20.44909668
10	Q13596	SNX1	21.8387661	23.32991982
11	Q14152	EIF3A	24.92718887	26.21811676
12	Q14696	MESD	19.84509277	21.00374222
13	Q14789	GOLGB1	24.66871452	23.57080078
14	Q15021	NCAPD2	0	20.3668766
15	Q15056	EIF4H	23.36826324	24.77660751
16	Q15075	EEA1	23.31741333	24.69104385
17	Q15233	NONO	24.7138195	25.76789665
18	Q16134	ETFDH	21.16029549	0
19	Q16513	PKN2	19.69333076	20.82150841
20	Q16658	FSCN1	25.69144249	26.86714554
21	Q16778	HIST2H2BE	26.90644264	25.62419128
22	Q16822	PCK2	22.51982117	24.02647972
23	Q16878	CDO1	0	23.31451225
24	Q5JRG1	NUP58	0	20.33123207
25	Q5T0I0	GSN	21.1754818	22.3467598
26	Q5VYK3	ECPAS	22.48892975	24.10093307
27	Q68CQ7	GLT8D1	0	21.56592941
28	Q68E01	INTS3	0	19.13560867
29	Q6P2E9	EDC4	19.89511681	21.12760925
30	Q7Z3U7	MON2	0	21.72558975
31	Q8IVF2	AHNAK2	21.0956459	0
32	Q8IWJ2	GCC2	20.04126358	21.07463455
33	Q8N129	CNPY4	19.50589371	0
34	Q8TBA6	GOLGA5	19.2819519	0
35	Q8TCT9	HM13	25.04963684	24.03355408
36	Q8TDD1	DDX54	0	19.40621758
37	Q8TEX9	IPO4	21.96370506	23.04977798
38	Q8WU90	ZC3H15	20.30273628	21.33576393
39	Q92575	UBXN4	0	20.73073959
40	Q92629	SGCD	0	19.04788017
41	Q92734	TFG	23.73055267	24.79872322
42	Q92882	OSTF1	20.70497513	21.89145088
43	Q96CG8	CTHRC1	21.28263092	22.5556221
44	Q96CT7	CCDC124	0	19.65881729
45	Q96JQ0	DCHS1	18.9074192	0
46	Q96SB3	PPP1R9B	21.21299934	0
47	Q96TA1	FAM129B	26.7624321	24.93035126

1	Q99715	COL12A1	25.5644474	27.04228592
2	Q99747	NAPG	0	20.63962364
3	Q99805	TM9SF2	21.15961838	20.02431679
4	Q99832	CCT7	25.16970634	26.43934822
5	Q9BPW8	NIPSNAP1	0	20.66440201
6	Q9BQ67	GRWD1	0	19.73229599
7	Q9BQS8	FYCO1	20.9930687	22.06111526
8	Q9BRF8	CPPED1	0	21.15165138
9	Q9BW60	ELOVL1	22.21208	21.1392746
10	Q9BY44	EIF2A	22.04266739	20.94713783
11	Q9H1B7	IRF2BPL	0	18.87306595
12	Q9H223	EHD4	0	20.26956558
13	Q9H2U2	PPA2	0	21.18507385
14	Q9HAV7	GRPEL1	20.83259964	22.38094521
15	Q9HB40	SCPEP1	0	20.93675232
16	Q9HCL0	PCDH18	0	19.58913612
17	Q9HD45	TM9SF3	22.06999016	20.69251251
18	Q9NRY4	ARHGAP35	0	19.44497871
19	Q9NSD9	FARSB	22.56020164	24.20329285
20	Q9NUQ8	ABCF3	0	19.8791523
21	Q9NV70	EXOC1	19.37553596	0
22	Q9NVI7	ATAD3A	22.91378593	24.31319809
23	Q9NW15	ANO10	0	20.39089584
24	Q9NX08	COMM8	0	20.09493828
25	Q9NXG2	THUMPD1	0	21.14413834
26	Q9NZB2	FAM120A	25.2062397	23.61717224
27	Q9ZNZ4	EHD2	25.39447212	26.43766594
28	Q9P2R3	ANKFY1	21.45848846	22.65425301
29	Q9UBG0	MRC2	23.40781975	24.75302315
30	Q9UH99	SUN2	19.84743309	21.2696228
31	Q9UL25	RAB21	21.68863487	22.91340256
32	Q9ULT8	HECTD1	0	20.53107643
33	Q9UMX0	UBQLN1	0	21.44955063
34	Q9UN70	PCDHGC3	0	20.26647949
35	Q9UNW1	MINPP1	0	20.22163963
36	Q9UQE7	SMC3	22.4522171	21.36420822
37	Q9Y224	RTRAF	22.34708405	23.44113731
38	Q9Y230	RUVBL2	23.94529915	24.95464706
39	Q9Y281	CFL2	0	21.72425652
40	Q9Y2X3	NOP58	0	21.9932766
41	Q9Y3I0	RTCB	23.71187782	24.85562134
42	Q9Y512	SAMM50	0	21.21240616
43	Q9Y5S2	CDC42BPB	19.38237	20.63794518
44	Q9Y5S9	RBM8A	21.61867332	20.58389473
45	Q9Y608	LRRFIP2	0	20.42070007
46	R4GNG3	GIT2	0	19.97084808
47	S4R3Z2	AKR1C3	21.77671814	0

Appendix Table 3

The antibodies, primers and protein used in the study.

Primary antibodies (Immunofluorescence)					
Antigen	Figure	Diluting factor	Company	Cat. No.	Batch No.
Notch 1 ICD	2D	1:200	e-Bioscience	14-5785-82	E04375-261
Total Notch1	2E	1:200	Cell Signalling	4380s	lot 2
Dll1	2F	1:200	R&D Systems	AF5026	
Osteopontin	2G	1:100	Dr Larry fisher (NIH)	LF-166 hOPN (C-terminus)	
Periostin	1C, 3H-J, App. 2A	1:400	Abcam	AB14041	
Notch 2 ICD	2E	1:200	Sigma	SAB4502022	410353
Lamin A/C	5B	1:200	Cell signalling	4777s	Lot 1
Lamin A/C	5E	1:200	Santa Cruz	sc-20681	A1116

Secondary antibodies (Immunofluorescence)				
Target	Dilution	Company	Cat. No.	Lot
Alexa 568 Donkey anti-Mouse IgG	1:500	Life Technologies	A10037	1303018
Alexa 568 Donkey anti-Rabbit IgG	1:500	Life Technologies	A10042	1964370
Alexa 568 Donkey anti-Rabbit IgG	1:500	Abcam	Ab175470	
Alexa 488 Donkey anti-Sheep IgG	1:300	Life Technologies	A11015	1322311
Alexa 488 Donkey anti-Mouse IgG	1:300	Life Technologies	A21202	1796361

Antibodies (Western Blotting)					
Antigen	Figure	Diluting factor	Company	Cat. No.	Batch No.
GapDH	5	1:500	Santa Cruz	SC-32233	H2114
Lamin A/C	5	1:400	Cell Signalling	4777	
Anti-Rabbit HRP	5	1:500	Cell Signalling	7074P2	
Anti-Mouse HRP	5	1:500	Cell Signalling	7076P2	

Primers			
Gene (mouse)	Forward primer ('5-'3)	Reverse primer ('5-'3)	PCR Product size

1	Hes1	TGAGCCAGCTGAAAACACTG	AGCACACTTGGGTCTGTGC	160
2	DLL1	GCACGGACCTCAAGTACTCC	ATGCTGCTCATCACATCCAG	200
3	Hey1	CTTTGGTGCATGGAAGTGT	CAGTCAGTGGAGGTCGTT	152
4	DLL4	GCGAGAAGAAAGTGGACAGG	ATTCTCCAGGTATGGCAAG	185
5	Jag1	ATCGTGCCTTCAGTT	ATTGCAGCCAAGGCCATAGT	234
6	Acta2	CAGATGTGGATCAGCAAACA	TGGCTAGGAATGATTGGAA	161
7	BGLAP	CAGCGAGGTAGTGAAGAG	GGGAAGAGGAAAGAAGGG	249
8	Runx2	CTCTGACCGCCTCAGTGATT	GGCTCAGGTAGGAGGGTAA	200
9	Periostin	CAAAACTGAAGGACCCACAC	TATTTCACAGGCACACTCCAT	154
10	Sparc	GTGCAGAGGAACCGAAGAG	AAGTGGCAGGAAGAGTCGAA	200
11	GapDH	ATCACTGCCACCCAGAACAC	CAGTGAGCTTCCCAGTCAG	148
12	36B4	GCAATGTTGCCAGTGTCTGT	GCCTTGACCTTTCAGCAAG	142
13	SPP1	TTGCAGTGATTGCTTTGC	GTCATGGCTTCGTTGGACT	200
14	Dlk1	GGCTTCATCGACAAGACCTG	CAGGTCTCGCACTTGTTGAG	185

Recombinant Proteins			
Protein	Company	Cat. No.	Lot
Human Jagged 1	R&D	1277-JG-050	RZL1713041